AN ABSTRACT OF THE THESIS OF

Ratikorn Netrabukkana for the degree of Master of Science in Chemical Engineering presented on November 4, 1994. Title: The Diffusion of Glucose and Glucitol in Microporous and Mesoporous Silica-based Catalysts.

Abstract approved: Redacted for Privacy

Gregory L. Rorrer

The diffusion and adsorption of glucose and glucitol in water-filled silica-based catalysts were studied under non-reaction conditions. Five silica-based catalysts with pore sizes ranging from 7.5 to 100 Å were considered, including HY-zeolite, Na-MCM-20, Na-MCM-41, silica gel-60, and silica gel-100. A liquid chromatographic technique was used to estimate the intracrystalline diffusivity (D_c) and the adsorption equilibrium constant (K) of glucose and glucitol in each catalyst.

Glucose and glucitol were non-adsorbed solutes because their values of K were below 1. The intracrystalline diffusivity of glucose and glucitol was significantly influenced by the pore diameter of the catalyst. For glucose, the value of D_c increased from 1.77×10^{-9} to 1.08×10^{-6} cm^2/sec when the pore diameter of the catalyst increased from 7.5 to 100 Å.

Although glucose and glucitol have almost the same molecular weight (180.2 vs. 182.2), the diffusivity of glucitol is two to four times lower than that of glucose because of molecular size and structure effects. In particular, glucitol has a larger critical diameter

than glucose, and so its diffusivity is lower. Furthermore, since glucitol is an ellipsoidal-shaped molecule, it has more difficulty passing through the pores than the spherical glucose molecule.

Two models reasonably predicted the intracrystalline diffusivity of glucose and glucitol in microporous and mesoporous silica-based catalysts as a function of reduced pore diameter λ (ratio between the solute diameter and the pore diameter):

1) $\log_{10}(D_c / D_m^0) = -0.52 - 8.52\lambda$

2) $\frac{D_c}{D_m^0} = \frac{(1-\lambda)^2}{1+620\lambda}$

where D_m^0 is the molecular diffusivity of the solute in the solvent at infinite dilution. Model 2 was recommended because it had a fundamental basis and only one adjustable parameter.

The Diffusion of Glucose and Glucitol in Microporous and Mesoporous Silica-based Catalysts

by

Ratikorn Netrabukkana

A THESIS

submitted to

Oregon State University

in partial fulfillment of
the requirements for the
degree of

Master of Science

Completed November 4, 1994
Commencement June 1995

Master of Science thesis of Ratikorn Netrabukkana presented on November 4, 1994

APPROVED:

Redacted for Privacy

Major Professor, representing Chemical Engineering

Redacted for Privacy

Chair of department of Chemical Engineering

Redacted for Privacy

Dean of Graduate School

I understand that my thesis will become part of the permanent collection of Oregon State University libraries. My signature below authorizes release of my thesis to any reader upon request.

Redacted for Privacy

Ratikorn Netrabukkana, Author

Table of Contents

Table of Contents (continued)

List of Figures

List of Figures (continued)

List of Figures (continued)

List of Tables

List of Appendix Tables

List of Appendix Tables (continued)

List of Appendix Tables (continued)

Nomenclature

c	concentration of the solute in the mobile phase (mg/mL)
c_e	equilibrium concentration of the solute in the mobile phase (mg/mL)
c_0	concentration of the solute in the injection sample (mg/mL)
c_p	concentration of the solute in catalyst pore (mg/mL)
d_p	diameter of the catalyst particle (cm)
$\overline{d}_p$	mean diameter of the catalyst particle (cm)
d_{pore}	pore diameter (Å)
$\overline{d}_{pore}$	mean pore diameter (Å)
$d_{pore,1}, d_{pore,2}$	lower and upper limits of integration in equation (4-1)
d_s	solute diameter (Å)
D_c	intracrystalline diffusion coefficient of the solute in catalyst micropores (cm^2/sec)
D_e	effective diffusion coefficient (cm^2/sec)
D_L	axial dispersion coefficient (cm^2/sec)
D_p	diffusion coefficient of the solute in catalyst macropores (cm^2/sec)
D_m^0	molecular diffusivity of the solute in the solvent at infinite dilution (cm^2/sec)

F_1	correction factor based on interaction of the solute molecule with the pore
F_2	correction factor based on interaction of the solvent molecule with the pore
$HETP$	height equivalent to a theoretical plate (cm)
k_f	external film mass transfer coefficient (cm/sec)
K	adsorption equilibrium constant (mL/mL)
L	length of packing (cm)
M_f	molecular weight of the solvent (g/gmol)
n	number of data points of equations (4-5) and (4-6)
P	adjustable parameter of equation (6-10)
Pe	Peclet number for mass transfer in the packed bed defined by equation 3-16 (dimensionless)
q^0	adsorption rate for a intraparticle diffusion limited process (mg/mL-sec)
r	radial position within the catalyst particle (cm)
r_c	radius of catalyst crystal (cm)
Re	Reynolds number defined by equation 3-23 (dimensionless)
R_p	radius of catalyst particle (cm)
S	N_2-BET surface area (m^2/g)
Sh	Sherwood number (dimensionless)
t	time (sec)

t_{in}	total injection time of the square input pulse (sec)
T	absolute temperature (K)
U	interstitial velocity (cm/min)
V_f	molal volume of solute at the normal boiling point (cm^3/gmol)
V_i	detector response (μV)
V_p	pore volume (mL/g)
W_i	weight fraction within size range $d_{pi} - d_{pi+1}$
z	distance along the column in axial direction (cm)

Greek Symbols

β	ratio between the distance from the pore wall in which solvent has altered viscosity and the overall radius
$\Delta\mu_w$	viscosity increment of solvent in the proximity of the pore wall (g/cm-sec)
ε	void fraction in the packed column (mL/mL)
ε_p	porosity of catalyst particle (mL/mL)
Φ_f	association parameter for the solvent (dimensionless)
Γ	square input pulse of the solute injected to the column (mg/mL)
λ	ratio between d_s and d_{pore} in equation (6-3)
μ	first moment of the response peak (min)
μ'	delay time of the peak with column removed (min)

μ_f	viscosity of the solvent (g/cm-sec)
ρ_f	density of the solvent (g/cm^3)
σ^2	second moment of the response peak (min^2)
$\sigma^{2'}$	variance of the peak with column removed (min^2)
τ	tortuosity

The Diffusion of Glucose and Glucitol in Microporous and Mesoporous Silica-based Catalysts

Chapter 1

Introduction and Literature Review

Many reaction, separation, and purification processes involve the diffusion and adsorption of solutes in liquid-filled porous solids. Examples of these processes which use glucose as the solute, water as the solvent, and silica-based catalysts as the porous solid include 1) the separation of fructose-glucose mixtures on CaY zeolite (Ho et al., 1987), and 2) the selective conversions of glucose to organic acids in Y-zeolite catalysts (Lourvanij and Rorrer, 1993) and pillared clay catalysts (Lourvanij and Rorrer, 1994).

Studies on liquid-phase diffusion and adsorption of solutes in porous solids have been ignored for a long time primarily because of the experimental difficulties associated with unsteady-state, batch methods for the diffusivity estimation. Recently, a new technique for estimating the diffusivity of solutes in liquid filled porous solids has been developed based on liquid chromatography (Ma and Lin, 1987; Ho et al., 1987; Awum et al., 1988; Ma and Lin, 1988; Ching, 1989; Uddin et al., 1990).

Ma and Lin (1987) proposed that the chromatographic technique has many advantages over batch methods. In particular, the chromatographic method obtains data simply, accurately, and rapidly using common HPLC equipment. In a HPLC system, the temperature is readily controlled or changed, and only small quantities of the solutes and catalysts are required. For very small particles, Lin and Ma (1989) proved that the

chromatographic technique was valid for particle diameters as small as 1-5 μm. The unsteady-state, batch methods are not valid for small particles, because the time to reach an equilibrium in a well-mixed tank is so fast that it is very difficult to take concentration vs. time data before reaching equilibrium.

The chromatographic method for diffusivity estimation uses a direct time domain analysis (Ma and Lin, 1987) or a moment analysis (Ho et al., 1987; Ma and Lin, 1988; Awum et al., 1988; Ching, 1989). Lin and Ma (1989) compared these two methods of analysis and found that the adsorption equilibrium constants and the diffusivities were comparable for the two methods. However, the moment method of analysis was mathematically simpler than the direct time domain analysis. Therefore this study will use the moment method of analysis to determine the adsorption equilibrium constant and the intracrystalline diffusivity by the chromatographic technique.

The diffusion of liquids in porous solids or solutes in liquid filled pores were studied in several different systems using the liquid chromatographic technique. Ma and Lin (1987) measured the intracrystalline diffusivities of methanol-H_2O, ethanol-H_2O, acetone-H_2O, toluene-C_6H_{14}, and acetone-C_6H_{14} in silicalite crystals. Awum et al.(1987) measured the intracrystalline diffusivities of phenol-H_2O, acetone-H_2O, bezene-C_6H_{12}, bezene-C_6H_{14}, and o-xylene-C_6H_{14} in 13X zeolite crystals. Also, Ching (1989) measured the diffusivities of glucose, maltose and maltotriose in silica gel. Finally, Uddin et al. (1990) measured the diffusivities of glutamine, methionine, phenylalanine and tryptophan in silica gel.

Satterfield et al.(1973) measured the diffusivities of 22 different solutes in large (3-4 mm) silica-alumina bead catalyst by using the unsteady-state method in a well mixed batch vessel.

Previous studies considered the effects of the size and chemical nature of the solute on the diffusivity within a single given catalyst. However, no one has considered the effect of pore size on the diffusivity of a single solute. If we measure the diffusivities of the same solute within catalysts of differing pore sizes, we can determine the effect of the pore size on the diffusivity.

The diffusion and adsorption of glucose in water-filled porous solids has been considered by some researchers. Satterfield et al.(1973) studied the adsorption and the diffusion of glucose in silica-alumina bead catalyst of 32 Å pore size at 25 ^{0}C, and found that glucose was a non-adsorbing solute with a diffusivity of 1.01×10^{-6} cm^2/sec. Ho et al. (1987) studied the adsorption of glucose in packed column of CaY zeolite catalyst at 29 ^{0}C and 60 ^{0}C, and showed that the isotherm for glucose was linear up to 25% wt. Furthermore, the adsorption equilibrium constants of glucose on CaY zeolite were 0.38 mL/mL at 29 ^{0}C and 0.44 mL/mL at 60 ^{0}C. Ho et al.(1987) concluded that glucose was a non-adsorbed solute, a result supported earlier by Satterfield et al.(1973).

Ching (1989) compared the diffusivities of glucose, maltose and maltotriose in silica gel of 27 Å pore size and found that as molecular weight of the solute increased, the diffusivity decreased. Uddin et al.(1990) also studied the effect of the molecular weight of the solute on the diffusivity, and obtained similar results. An interesting point about the diffusivity measurements is that the solute configuration can affect the diffusivity. Solutes

with almost the same molecular weight but have different structures may have a significant difference in their diffusivities.

Two models were developed for the prediction of the diffusivity of liquids in porous solids. One was proposed by Satterfield et al.(1973), and the other was proposed by Ternan (1987). These two models will be used for the development of a model to predict the diffusivity of glucose and glucitol in microporous and mesoporous silica-based catalysts as a function of pore diameter.

Chapter 2

Research Objectives

Fundamental studies of diffusion and adsorption of glucose in water-filled silica-based catalysts under non-reaction conditions are essential to the development of new technologies for the shape-selective conversion of glucose to organic chemicals in microporous and mesoporous molecular sieving catalysts. Therefore the objectives of this study are:

1) To assess the suitability of the chromatographic technique for estimating the intracrystalline diffusivity of glucose and glucitol in water-filled silica-based catalysts;

2) To measure the intracrystalline diffusivity and the adsorption equilibrium constant of glucose and glucitol in five different microporous and mesoporous silica-based catalysts ranging from 7.5 to 100 Å in pore diameter;

3) To compare the diffusivity of glucose, a cyclic six-carbon sugar, to glucitol, a linear six-carbon sugar as a function of catalyst pore diameter from 7.5 to 100 Å;

4) To develop a model for predicting the intracrystalline diffusivity of glucose and glucitol in microporous and mesoporous silica-based catalysts as a function of pore diameter from 7.5 to 100 Å.

Chapter 3

Mathematical Analysis

The determination of the intracrystalline diffusion coefficient of glucose in molecular sieving catalysts by the chromatographic method requires a mathematical model. Intracrystalline diffusion, axial dispersion and adsorption processes are considered in the modeling of a column packed with catalyst particles, as illustrated in Figure 1. The mass balance over a differential element of the packed column results in two partial differential equations. One describes the mass transfer of the solute in the mobile phase of the column, and the other describes the intracrystalline diffusion of the solute within the porous catalyst. The mathematical model is based on the following assumptions:

1) Uniform solute concentration profile in the mobile liquid phase along the radial direction of the column due to a small ratio of column diameter to column length;
2) Constant interstitial velocity of liquid down the length of the column;
3) Spherical catalyst particles with a uniform particle size;
4) Linear isotherm for the adsorption of the solute on the catalyst;
5) Isothermal system;
6) No chemical reaction.

The differential mass balance of the solute in the mobile phase is given by

$$\frac{\partial c}{\partial t} + U\frac{\partial c}{\partial z} + \left(\frac{1-\varepsilon}{\varepsilon}\right)q^0 = D_L\frac{\partial^2 c}{\partial z^2} \qquad (3\text{-}1)$$

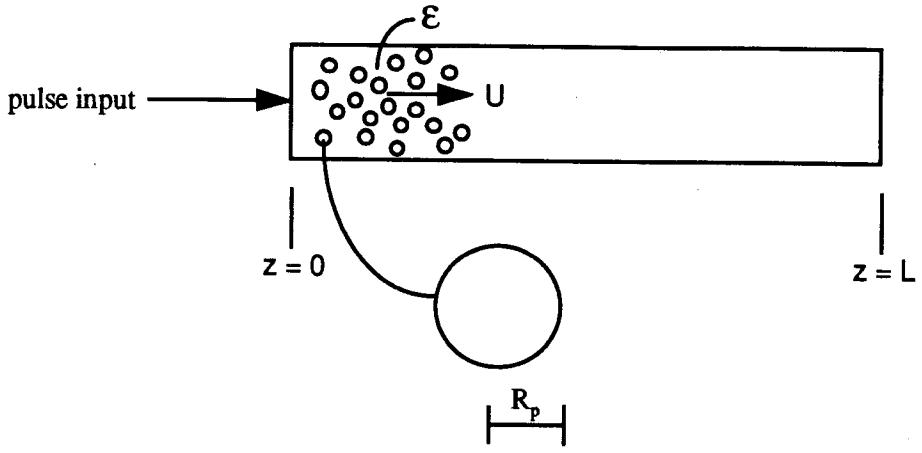

Figure 1. The packed column.

where c is the concentration of the solute in the mobile phase at position z (mg/mL), U is the interstitial velocity (cm/sec), ε is the void fraction in the packed column (mL/mL), q^0 is the adsorption rate on catalyst particle surface (mg/mL-sec), D_L is the axial dispersion coefficient (cm^2/sec), t is time (sec), and z is the distance along the column in axial direction (cm). The adsorption rate q^0 (mg/mL-sec) is represented by

$$q^0 = D_c \frac{3}{R_p} \frac{\partial c_p}{\partial r}\bigg|_{r=R_p} \qquad (3\text{-}2)$$

where R_p is the radius of catalyst particle (cm), C_p is the concentration of the solute in catalyst pore (mg/mL), and D_c is the intracrystalline diffusion coefficient of the solute (cm^2/sec).

When pure solvent flows through the packed column, the initial condition is

$$c(z,t) = 0 \qquad \text{at t} = 0 \qquad (3\text{-}3)$$

for the mobile phase. The boundary condition at the inlet of the column is given by

$$c = \Gamma + \frac{D_L}{U}\frac{\partial c}{\partial z} \qquad \text{at z} = 0 \qquad (3\text{-}4)$$

and the boundary condition at the outlet of the column is given by

$$\frac{\partial c}{\partial z} = 0 \qquad \text{at z} = \text{L} \qquad (3\text{-}5)$$

In equation (3-4) Γ is the square input pulse of the solute injected to the column at z = 0, and is defined as

$$\Gamma = \begin{cases} c_0 & 0 \le t \le t_{in} \\ 0 & t > t_{in} \end{cases} \qquad (3\text{-}6)$$

where c_0 is the concentration of the solute in the injection sample (mg/mL), and t_{in} is the total injection time of the square input pulse (sec).

The differential mass balance of the solute within a single, spherical catalyst particle is given by

$$D_c\left(\frac{\partial^2 c_p}{\partial r^2}+\frac{2}{r}\frac{\partial c_p}{\partial r}\right)=\varepsilon_p\frac{\partial c_p}{\partial t} \qquad (3\text{-}7)$$

where ε_p is the porosity of catalyst particle (mL/mL) and r is the radial position within the catalyst particle (cm).

For a given catalyst particle, the initial condition is

$$c_p(z,r,t)=0 \qquad \text{at } t=0 \qquad (3\text{-}8)$$

and the boundary conditions are

$$\frac{\partial c_p}{\partial r}=0 \qquad \text{at } r=0 \qquad (3\text{-}9)$$

and

$$\frac{\partial c_p}{\partial r}=\frac{k_f}{D_c}(c-c_e) \qquad \text{at } r=R_p \qquad (3\text{-}10)$$

with $c_p = Kc_e$ at $r = R_p$. In equation (3-10), k_f is the external film mass transfer coefficient (cm/sec), c_e is the equilibrium concentration of the solute in the mobile phase (mg/mL), and K is the adsorption equilibrium constant (mL/mL).

When the adsorption equilibrium of the solute on the catalyst follows a linear isotherm, the analytical solution of the model equation (3-1) can generally be obtained in the Laplace domain. However inversion of the transform to obtain the time domain solution is difficult and the resulting expression is cumbersome. The moment analysis avoids this difficulty and allows the determination of model parameters directly by matching experimental response curves without recourse to the time domain solution.

Moment Analysis

The expressions for the moments of the pulse response of the solute can be derived directly from the solution of the model equations in Laplace form, by application of van der Laan's Theorem (van der Laan, 1958). The first moment (μ) is

$$\mu \equiv \bar{t} = \frac{\int_0^\infty ctdt}{\int_0^\infty cdt} = -\lim_{s\to 0} \frac{\partial \tilde{c}}{\partial s} \frac{1}{c_0} \qquad (3\text{-}11)$$

and the second moment (σ^2) is

$$\sigma^2 \equiv \frac{\int_0^\infty c(t-\mu)^2 dt}{\int_0^\infty cdt} = \lim_{s\to 0} \frac{\partial^2 \tilde{c}}{\partial s^2}\left(\frac{1}{c_0}\right) - \mu^2 \qquad (3\text{-}12)$$

The expressions for the first and second moments for a packed chromatography column, which include axial dispersion, external film mass transfer, macropore diffusion, and micropore diffusion are detailed by Haynes and Sarma (1973). Specially, the first moment (μ) is given by

$$\mu \equiv \frac{L}{U}\left[1+\frac{(1-\varepsilon)}{\varepsilon}K\right] \qquad (3\text{-}13)$$

The HETP (height equivalent to a theoretical plate) is obtained from the first moment (μ) and second moment (σ^2) by

$$HETP = \frac{\sigma^2}{\mu^2}L = 2\frac{D_L}{U} + 2U\left(\frac{\varepsilon}{1-\varepsilon}\right)\left\{\frac{R_p}{3k_f} + \frac{R_p^2}{15\varepsilon_p D_p} + \frac{r_c^2\left(K-\varepsilon_p\right)}{15K^2 D_c}\right\}\left\{1+\frac{\varepsilon}{(1-\varepsilon)K}\right\}^{-2} \qquad (3\text{-}14)$$

where L is the length of packed column (cm), D_p is the diffusion coefficient of the solute within the catalyst macropores (cm^2/sec), and r_c is the crystal radius (cm).

From equation (3-14), the contributions of the axial dispersion term and three mass transfer resistance terms are linearly additive. The model is simplified by dropping the terms which are considered negligible. In particular, for microporous catalysts, the macropore diffusion term is dropped and equation (3-14) reduces to

$$HETP = \frac{\sigma^2}{\mu^2} L = 2\frac{D_L}{U} + 2U\left(\frac{\varepsilon}{1-\varepsilon}\right)\left\{\frac{R_p}{3k_f} + \frac{R_p^2\left(K-\varepsilon_p\right)}{15K^2 D_c}\right\}\left\{1+\frac{\varepsilon}{(1-\varepsilon)K}\right\}^{-2} \quad (3\text{-}15)$$

In equation (3-15), the crystal radius (r_c) is now the particle radius (R_p) if the catalyst particles are not sintered into a pellet.

Lin and Ma (1989) suggested that the axial dispersion coefficient (D_L) in equation (3-15) can be calculated by the following equation proposed by Wen and Fan (1975)

$$Pe = \frac{0.20}{\varepsilon} + \frac{0.011}{\varepsilon}\mathrm{Re}^{0.48} \quad (3\text{-}16)$$

The Peclet number (Pe) for the liquid in the packed bed is approximately independent of liquid velocity at low fluid velocities. Thus, D_L is calculated from the Peclet number by

$$D_L = \frac{Ud_p}{Pe} \quad (3\text{-}17)$$

where d_p is the diameter of the catalyst particle (cm). Substitution of equation (3-17) into equation (3-15) yields the following simplified equation for the HETP

$$HETP = A + BU \quad (3\text{-}18)$$

where A and B are constants, defined by

$$A = \frac{2d_p}{Pe} \qquad (3\text{-}19)$$

and

$$B = 2\left(\frac{\varepsilon}{1-\varepsilon}\right)\left\{\frac{R_p}{3k_f} + \frac{R_p^2\left(K-\varepsilon_p\right)}{15K^2D_c}\right\}\left\{1+\frac{\varepsilon}{(1-\varepsilon)K}\right\}^{-2} \qquad (3\text{-}20)$$

At very low Reynolds numbers ($0.0015 < Re < 55$), the external film mass transfer coefficient k_f can be calculated from the Sherwood number (Sh) by the following correlation (Wilson and Geankoplis, 1966)

$$Sh = \frac{1.09}{\varepsilon}\mathrm{Re}^{0.33}\,Sc^{0.33} \qquad (3\text{-}21)$$

The Sherwood number (Sh) is defined as

$$Sh = \frac{2R_p k_f}{D_m^0} \qquad (3\text{-}22)$$

The Reynolds number (Re) is represented by

$$\mathrm{Re} = \frac{\rho_f \varepsilon U d_p}{\mu_f} \qquad (3\text{-}23)$$

The Schmidt number (Sc) is represented by

$$Sc = \frac{\mu_f}{\rho_f D_m^0} \qquad (3\text{-}24)$$

where D_m^0 is the molecular diffusivity of the solute in the solvent at infinite dilution (cm^2/sec), ρ_f is the density of the solvent (g/cm^3) and μ_f is the viscosity of the solvent (g/cm-sec). It is reasonable to estimate k_f using the average liquid velocity because the term $\frac{R_p^2(K-\varepsilon_p)}{15K^2D_c}$ is much greater than the term $\frac{R_p}{3k_f}$ in equation (3-15). Thus, the constant B is essentially independent of the liquid velocity.

The adsorption equilibrium constant (K) and the intracrystalline diffusion coefficient (D_c) are determined from μ and σ^2 vs. U data for a given temperature. From equation (3-13), K is obtained directly from a slope of μ vs. 1/U. The term D_c is obtained directly from the slope of HETP vs. U data in the linear region, given K, and estimates for k_f, R_p, ε_p and ε.

Chapter 4

Experimental

Materials

The hexose sugar (D)-glucose ($C_6H_{12}O_6$) and the linear polyhydroxy alcohol (D)-glucitol ($C_6H_{14}O_6$) used in this study were obtained from Sigma Chemical Company. The molecular weight of glucose is 180.2 vs.182.2 for (D)-glucitol. Their molecular structures are given in Figures 2 and 3 respectively.

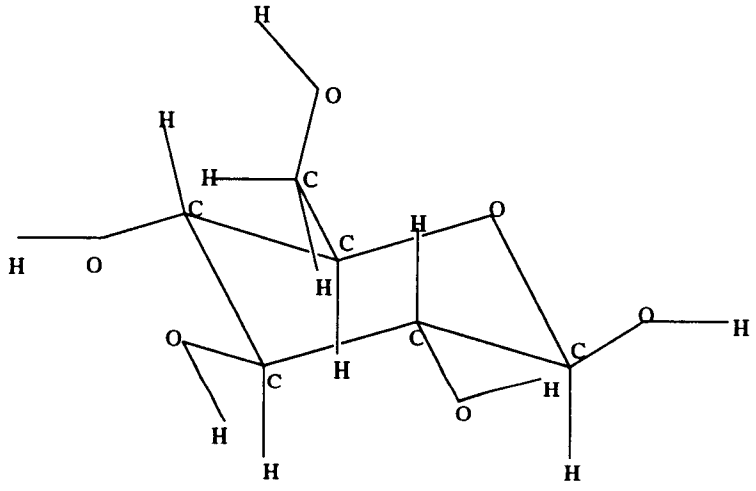

Figure 2. Molecular structure of (D)-glucose.

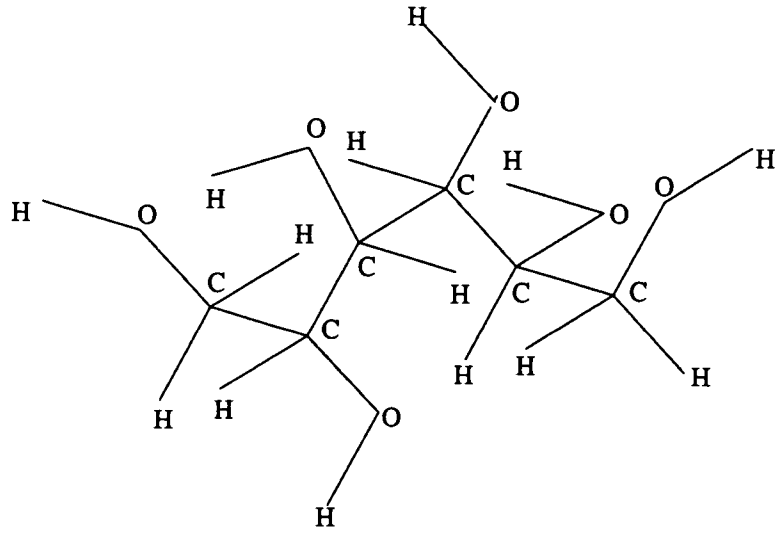

Figure 3. Molecular structure of (D)-glucitol.

The molecular dimensions of (D)-glucose and (D)-glucitol were computed using Hyperchem Software (Version 2, Autodesk, Inc.). The critical dimensions of each compound were determined from the least-hindered conformation using bond angles, bond lengths, atomic and Van der Waals radii (for details see appendix A). The largest long axis and short axis of (D)-glucose and (D)-glucitol are provided in Table 1.

Table 1. Molecular dimensions.

Molecule	Long Axis (Å)		Short Axis (Å)	
	Atomic Radii	Van der Waals Radii	Atomic Radii	Van der Waals Radii
Glucose	7.665	8.583	7.5	8.417
Glucitol	8.797	9.714	7.084	8.001

Five silica-based porous materials with nominal pore size ranging from 7.5 to 100 Å were used in this study, as summarized in Table 2.

Table 2. Silica-based porous materials.

Catalyst	Material	Nominal Pore size (Å)
HY-zeolite	aluminosilicate	7.5
Na-MCM-20	aluminosilicate	25
Na-MCM-41	aluminosilicate	40
silica gel-60	silica	60
silica gel-100	silica	100

The silica gel-100 and silica gel-60 were obtained from Aldrich Chemical Company, and HY-zeolite catalyst was obtained from the PQ Catalyst Corporation. The Na-MCM-41 and Na-MCM-20 molecular sieves were synthesized in the laboratory, as described next.

Synthesis of Na-MCM-41 and Na-MCM-20 Mesoporous Molecular Sieves

The liquid crystal templating technique (Beck et al, 1992) was used in the synthesis of the Na-MCM-41 and Na-MCM-20 mesoporous molecular sieves. The preparation of Na-MCM-41 is explained below.

Prior to templating, 29% wt cetyltrimethylammonium chloride surfactant solution ($C_{16}H_{33}(CH_3)_3NCl$, Pfaltz & Bauer Inc.) was exchanged with IRA-400 (OH) resin (4meq /g, Sigma Chemical Company) in a well mixed beaker to prepare the hydroxide form of the surfactant cation. Then, 100 g $C_{16}H_{33}(CH_3)_3NOH/Cl$, 2.2 g sodium aluminate (Pfaltz & Bauer Inc.), 50 g tetramethyl ammonium silicate (0.5 TMA/SiO_2, 10% wt silica, SACHEM Inc.), and 12.5g HiSil (PPG Inc.) were combined together and stirred at 350 rpm and 120 °C in a 300 mL Parr autoclave for 24 hours. After cooling, the solid fraction was vacuum-filtered from the slurry, washed with distilled water, and then dried in air at room temperature. The air-dried solid was calcined at 540 °C in flowing N_2 for 1 hour and then in flowing air for 6 hours.

The preparation of Na-MCM-20 was exactly the same as Na-MCM-41 synthesis explained above except for the surfactant cation. In this preparation, 50% dodecyltrimethyl ammonium chloride ($C_{12}H_{25}(CH_3)_3NCl$, Pfaltz & Bauer Inc.) was substituted for $C_{16}H_{33}(CH_3)_3NCl$.

Surface Area, Pore Volume and Pore Size Distribution Measurements

The surface area, pore volume, and pore size distribution of each catalyst was measured on a Micromeretics ASAP-2000 surface area and porosimetry analysis system. The BET surface area and pore volume of all catalysts were determined by static nitrogen physisorption at 77 K.

For Na-MCM-41, Na-MCM-20 and HY-zeolite, the pore size distribution was determined by pore-filling with increasing partial pressure of argon at 87.3 K. The pore

diameter was estimated by the Horvath-Kawazoe method of analysis (1983) which assumes the pores have a slit geometry.

For the silica gel-100 and silica gel-60, the pore size distribution was determined by pore-filling with increasing partial pressure of nitrogen at 77 K. The pore diameter was calculated by BJH method (Barrett et al., 1951) based on the desorption model and desorption data.

Pore size distributions of each catalyst are shown in Figures 4 to 8.

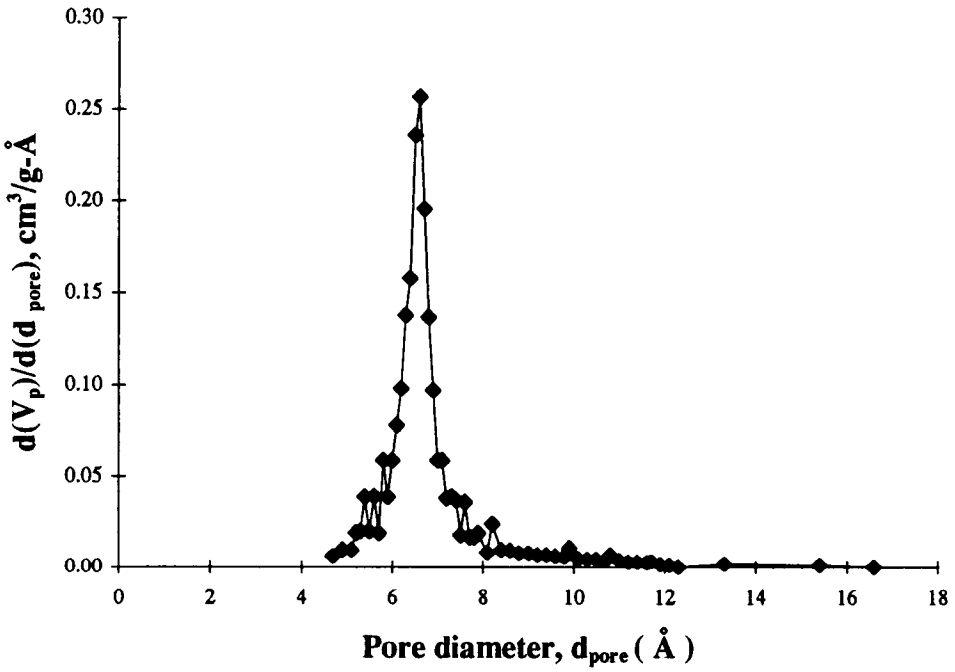

Figure 4. Pore size distribution of HY-zeolite.

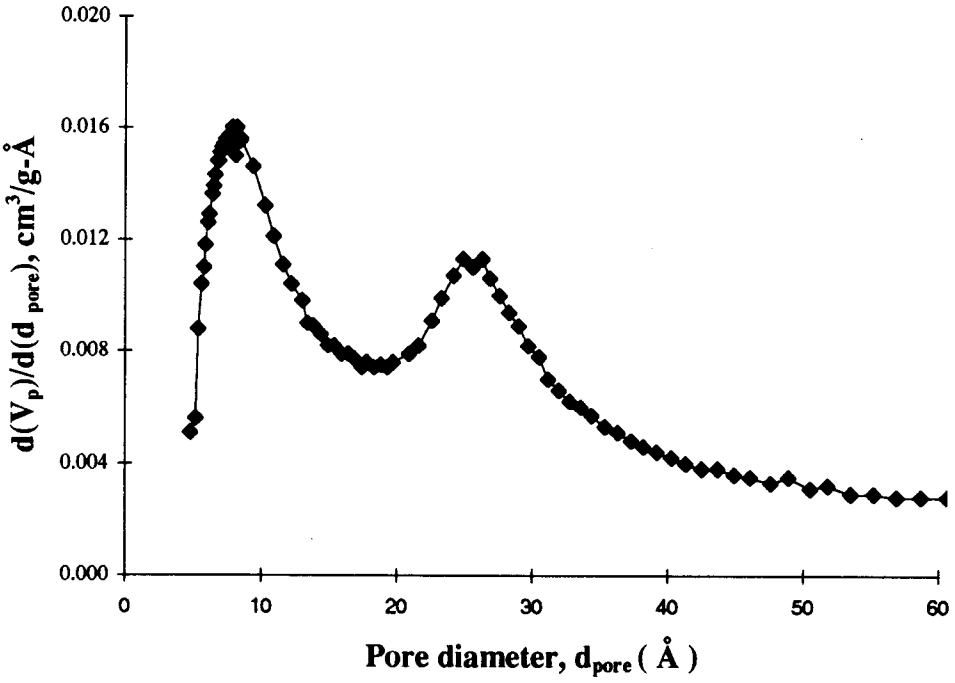

Figure 5. Pore size distribution of Na-MCM-20.

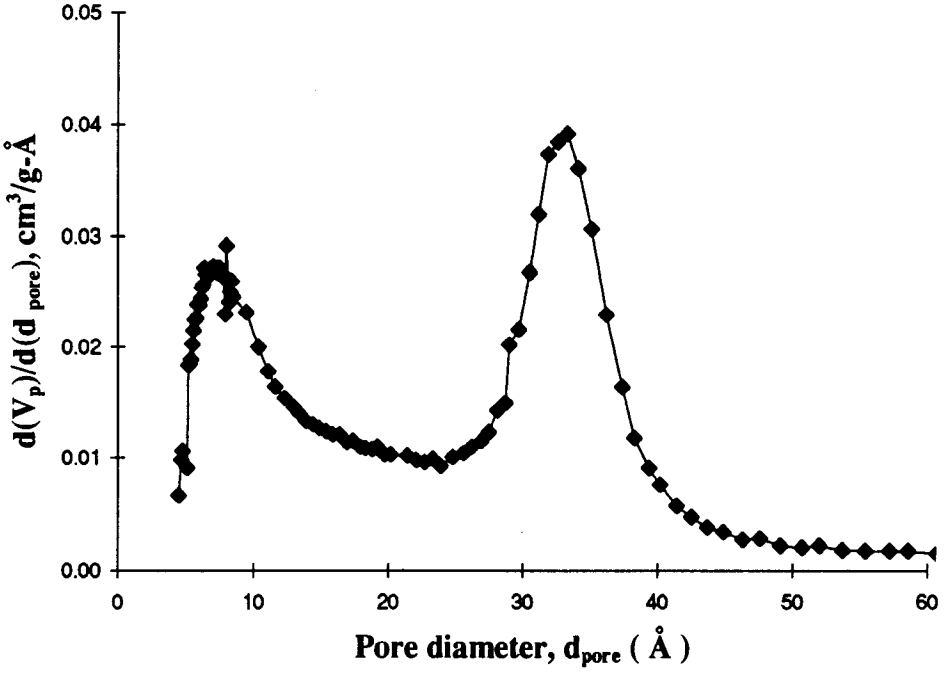

Figure 6. Pore size distribution of Na-MCM-41.

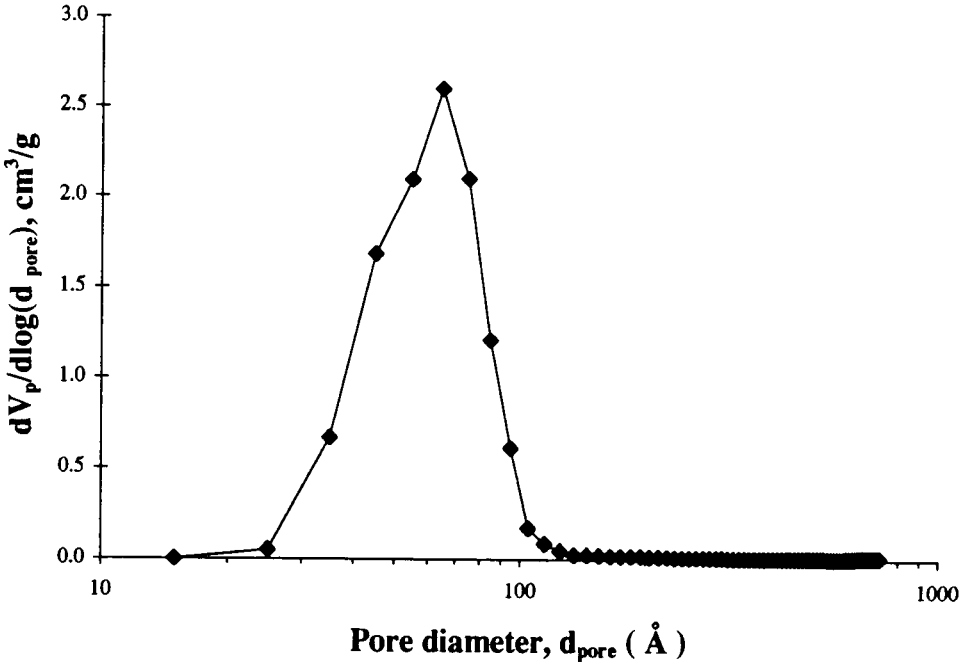

Figure 7. Pore size distribution of silica gel-60.

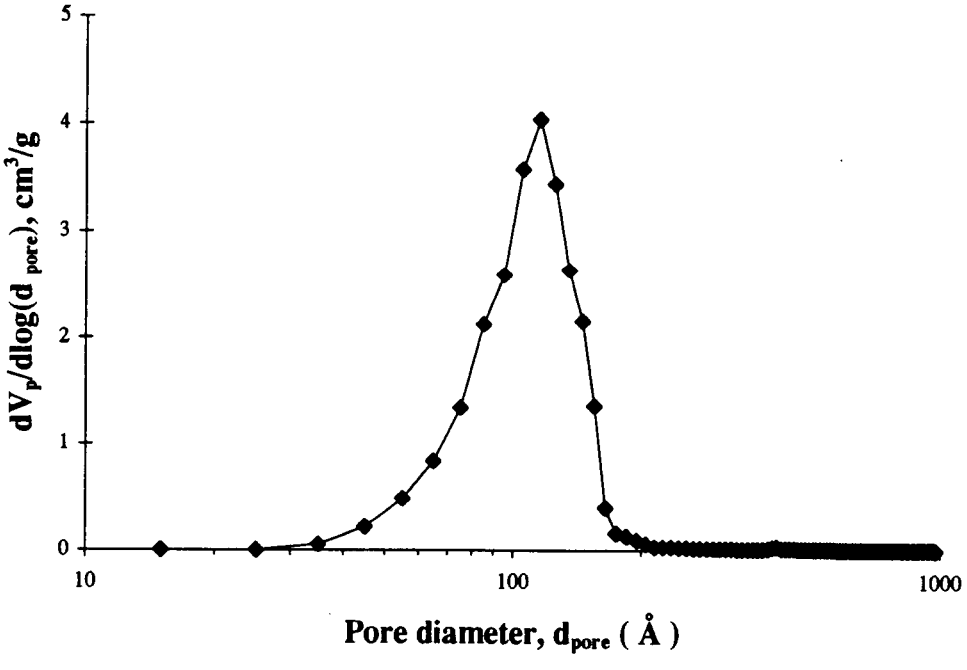

Figure 8. Pore size distribution of silica gel-100.

The mean pore size ($\overline{d}_{pore}$) for each catalyst was computed by trapezoid rule numerical integration of

$$\overline{d}_{pore} = \frac{\int_{d_{pore,1}}^{d_{pore,2}} d_{pore} f(d_{pore}) \mathrm{d}(d_{pore})}{\int_{d_{pore,1}}^{d_{pore,2}} f(d_{pore}) \mathrm{d}(d_{pore})} \qquad (4\text{-}1)$$

where $f(d_{pore})$ is the pore size distribution function, and $d_{pore,1}$ and $d_{pore,2}$ are the limits of integration corresponding to the pore size range of interest.

Particle Size Distribution

Before particle size distribution measurements, the silica gel-100 and silica gel-60 were sieved into the range of 53-100 μm while Na-MCM-41, Na-MCM-20 and HY-zeolite were sieved into the range of 20-53 μm. A HORIBA CAPA-700 centrifugal automatic particle size distribution analyzer was used to measure the particle size distribution of each sieved catalyst using a non-contact method based on liquid-phase sedimentation, where the particle concentration (weight fraction) was measured based on the light transmitted through the solution. The particle size distribution of each of the five catalysts are shown in Figures 9 to 13.

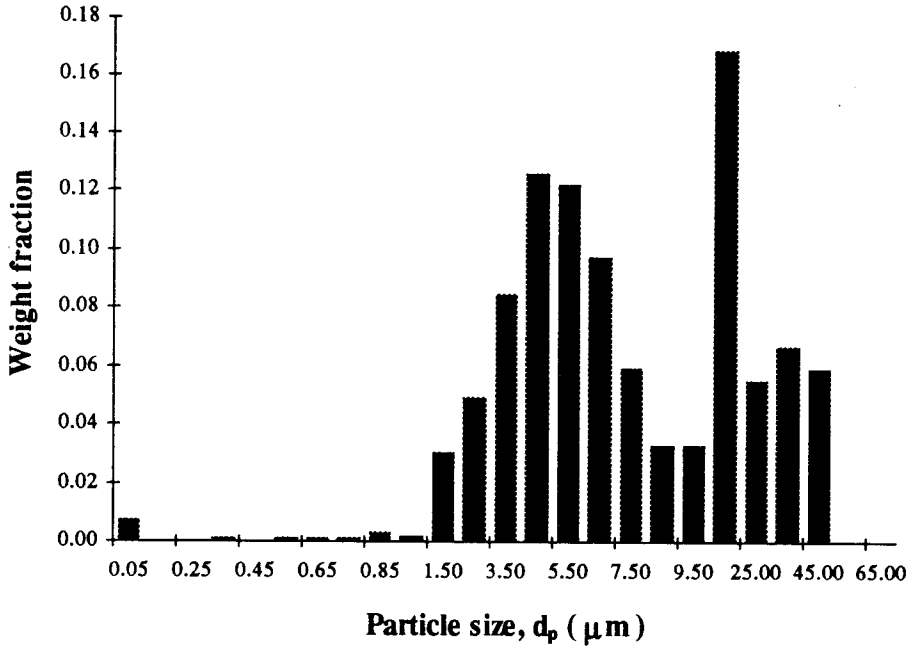

Figure 9. Particle size distribution of HY-zeolite.

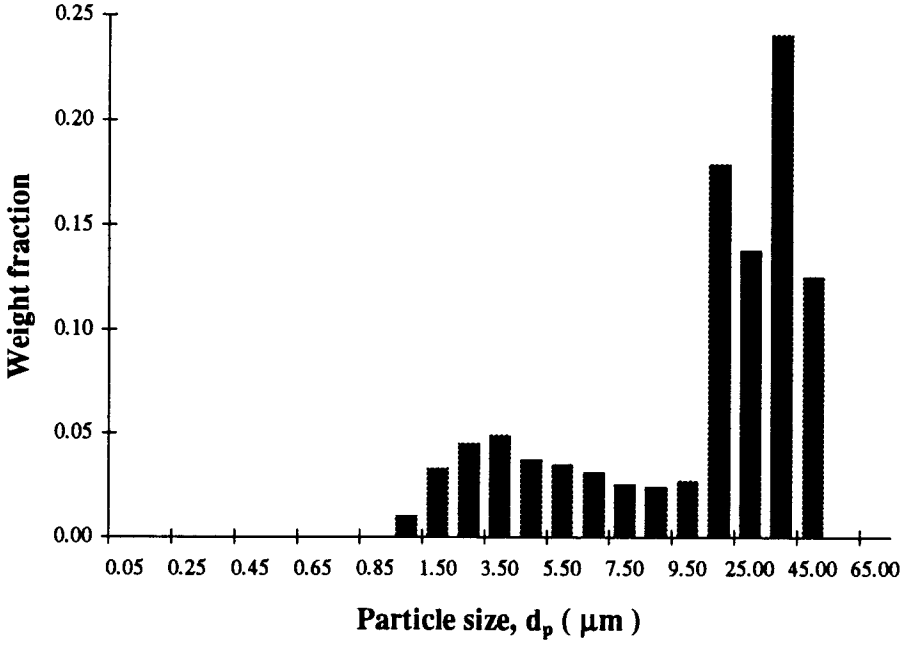

Figure 10. Particle size distribution of Na-MCM-20.

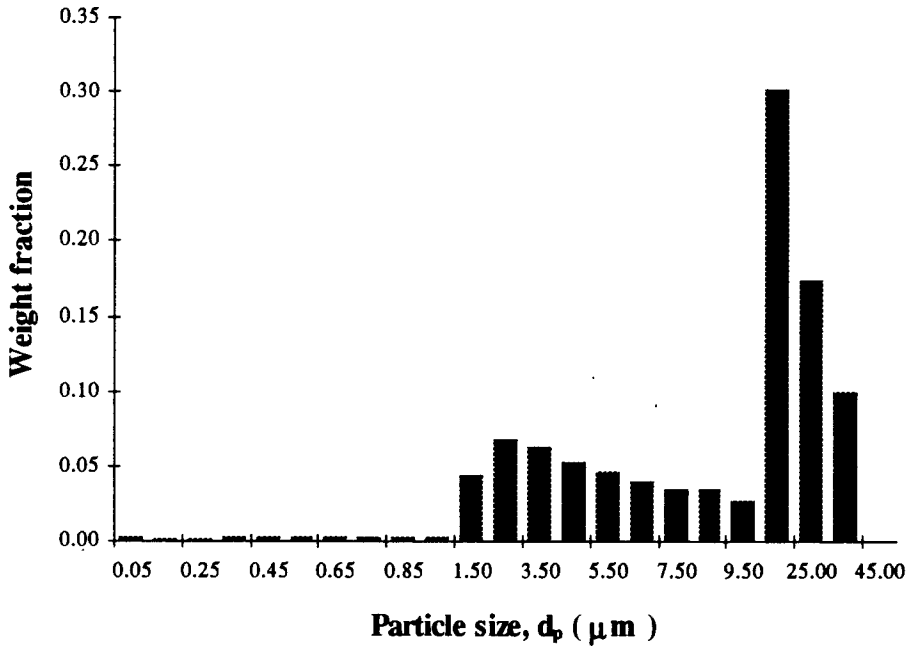

Figure 11. Particle size distribution of Na-MCM-41.

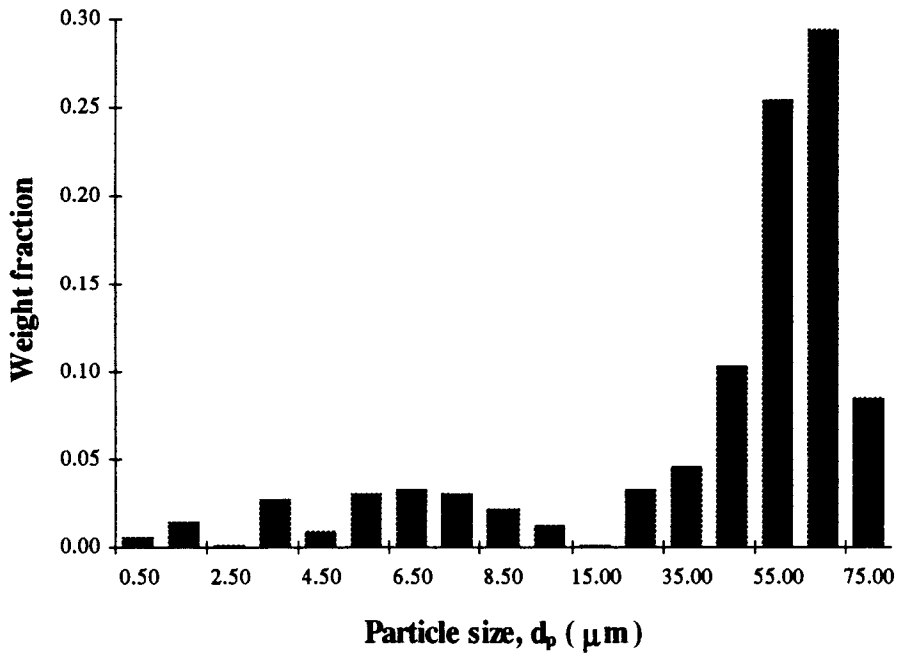

Figure 12. Particle size distribution of silica gel-60.

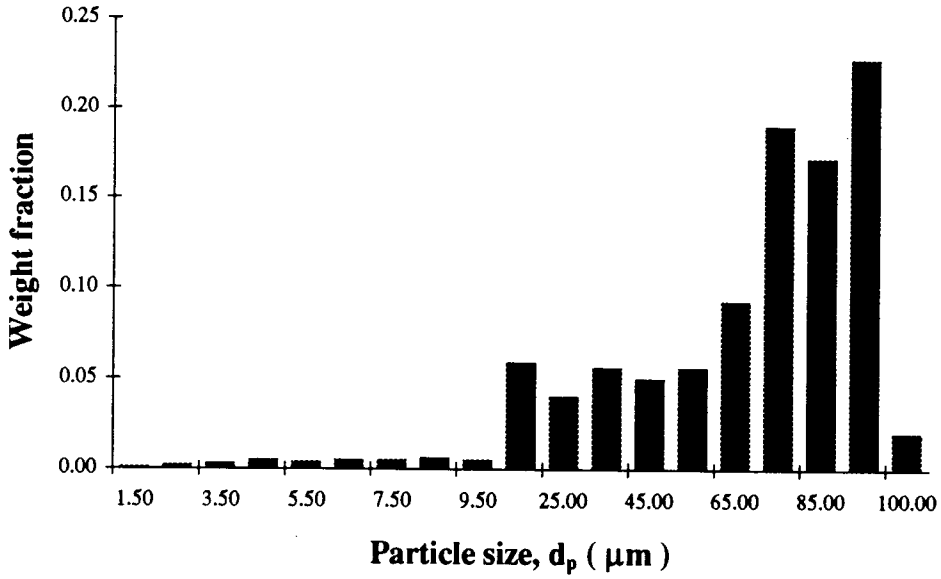

Figure 13. Particle size distribution of silica gel-100.

The mean particle size ($\bar{d}_p$) for each catalyst was computed by three methods:

1. Weighted Average

$$\bar{d}_p = \sum_{\text{all size}} d_{pi} W_i \qquad (4\text{-}2)$$

2. Weighted Integral Average

$$\bar{d}_p = \frac{\int_0^\infty d_p W \mathrm{d}(d_p)}{\int_0^\infty W \mathrm{d}(d_p)} \qquad (4\text{-}3)$$

3. Surface Average

$$\bar{d}_p = \frac{1}{\sum_{\text{all size}} \left(\frac{W_i}{d_{pi}} \right)} \qquad (4\text{-}4)$$

In equations (4-2) to (4-4) W_i is the weight fraction within size range d_{pi} to d_{pi+1}. The results of the mean particle size calculations for each method are presented in Table 3.

Table 3. Mean particle size.

Catalyst	Mean particle size ($\bar{d}_p$, μm)		
	Weighted Average	Weighted Integral Average	Surface Average
HY-zeolite	12.29	23.71	3.18
Na-MCM-20	21.79	29.68	8.33
Na-MCM-41	14.37	21.96	4.61
silica gel-60	47.67	52.86	15.85
silica gel-100	67.98	63.01	40.52

The values for $\bar{d}_p$ computed by the Surface Average method did not agree with the particle size distributions shown in Figures 9-13. Therefore, the Surface Average

method was not used. When the other two methods (Weighted Average and Weighted Integral Average methods) were compared, the Weighted Integral Average method provided the least truncation error of integration. Therefore the Weighted Integral Average method was selected for the final analysis of data.

Summary of Catalyst Parameters

The catalyst parameters are summarized in Table 4.

Table 4. Catalyst parameters.

Catalyst	Mean pore diameter, $\overline{d}_{pore}$ (Å)	Limits of Integration[a] (Å)	Pore volume, V_p[b] (mL/g)	N_2-BET surface area, S (m^2/g)	Mean particle size, $\overline{d}_p$ (μm)	Void fraction in packed bed, ε
HY-zeolite	6.83	4.90-11.9	0.24	515.2	23.7	0.27
Na-MCM-20	27.37	18.3-39.2	1.11	541.8	29.7	0.37
Na-MCM-41	32.81	18.3-60.7	1.39	799.8	22.0	0.38
silica gel-60	66.40	15-195	0.76	407.8	52.9	0.30
silica gel-100	116.10	15-395	1.02	313.2	63.0	0.33

(a) corresponding to the pore size range of interest.
(b) by N_2 pore filling.

Apparatus and Procedures

The diffusion measurements by the Method of Moments were carried using a High Performance Liquid Chromatography (HPLC) system, which consisted of a Waters 501 isocratic solvent pump, an Eldex column oven, a 20 μL Rheodyne 725 injector valve, and an Altex 156 refractive index (RI) detector. The RI detector was interfaced to an AST-286 computer equipped with Peak Simple II chromatography Software and AD board (SRI, Inc.). The HPLC system is schematically shown in Figure 14.

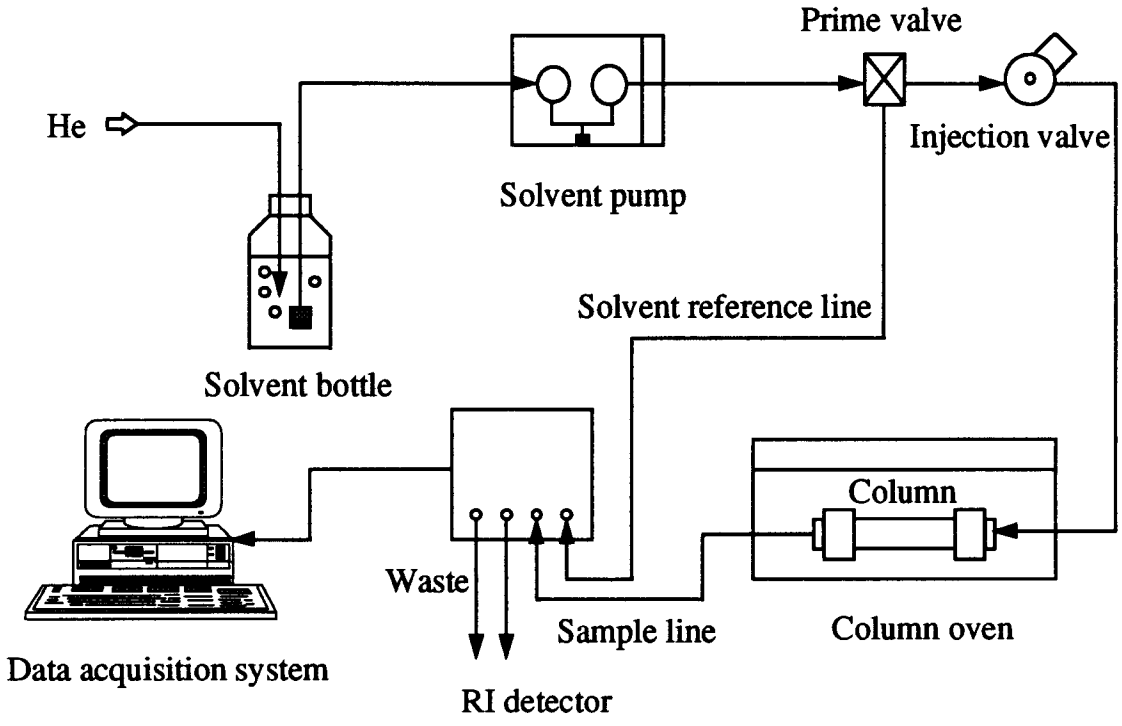

Figure 14. High Performance Liquid Chromatography (HPLC) system.

The column shown in Figure 15 consists of a stainless-steel tube with zero-dead volume column end fittings (Upchurch Scientific, Inc.). A wire mesh screen within the column end fittings retains the catalyst. The inner diameter (ID) of the column is 0.457 cm and the length (L) of packing is 10 cm.

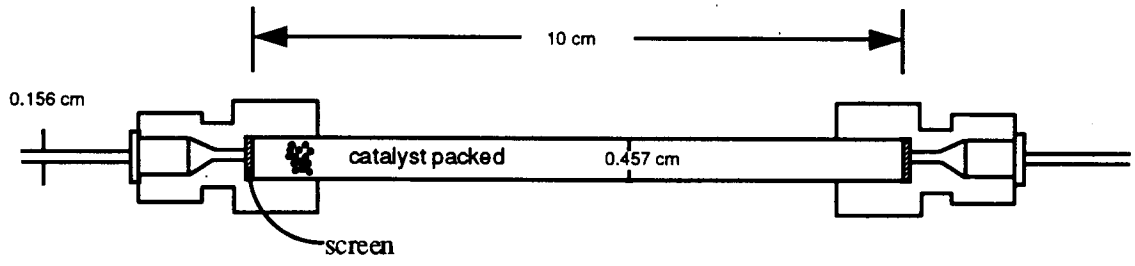

Figure 15. Schematic packed catalyst column.

The silica gel-100 and silica gel-60 were sieved into the range of 53-100 μm while Na-MCM-41, Na-MCM-20 and HY-zeolite were sieved into the range of 20-53 μm. Each column was packed with sieved catalyst by a dry packing method, in which the catalyst powder was added to the column in serial increments (typically 5 mg powder per increment). Between increments, the column was gently tapped on a hard surface to settle the catalyst and to ensure uniform packing of the catalyst powder within the column. The mass of the packed catalyst was measured. The packed column was connected to the HPLC system, and solvent (HPLC grade water) at 0.1 mL/min was pumped through the column packing. In order to remove residual gases within the catalyst pores, the column was heated to 70 ^{0}C for 2 hours under a solvent flow of 0.1 mL/min. The column was

then allowed to cool back down to 30 ^{0}C for 12 hours under a solvent flow of 0.1 mL/min.

The HPLC Experimental Parameters for Response Peak Measurements

For measurement of the response peak of a given flow rate, the 20 μL injection sample loop was first loaded with a sample solution of a given solute concentration using a syringe. The sample was then injected into the column, and the RI detector response vs. time data were recorded by the computer data acquisition system at a rate of 60 samples per minute. The response peak was obtained for five flow rates: 0.1, 0.2, 0.3, 0.4 and 0.5 mL/min. The temperature was maintained at 30 ^{0}C. The HPLC experimental parameters are shown in Table 5.

Table 5. HPLC experimental parameters

Temperature	30 °C
Column diameter	4.57 mm
Column length	10 cm
Flow rate range	0.1-0.5 mL/min
Initial solute concentration [a]	50 mg/mL
Volume of sample injected	20 µL
Mode of detection, range	Differential Refractive Index (DRI), range = 4x

(a) Solutes were glucose or glucitol.

The detector response vs. time data were used for the analysis of first and second moments. The first moment (μ) and second moment (σ^2) were numerically evaluated by the Trapezoid Rule using

$$\mu = \frac{\int_0^\infty ctdt}{\int_0^\infty cdt} = \frac{\sum_{i=1}^{n} c_i t_i \Delta t_i}{\sum_{i=1}^{n} c_i \Delta t_i} = \frac{\sum_{i=1}^{n} V_i t_i \Delta t_i}{\sum_{i=1}^{n} V_i \Delta t_i} \qquad (4\text{-}5)$$

$$\sigma^2 = \frac{\int_0^\infty c(t-\mu)^2 dt}{\int_0^\infty cdt} = \frac{\sum_{i=1}^{n} c_i (t_i-\mu)^2 \Delta t_i}{\sum_{i=1}^{n} c_i \Delta t_i} = \frac{\sum_{i=1}^{n} V_i (t_i-\mu)^2 \Delta t_i}{\sum_{i=1}^{n} V_i \Delta t_i} \qquad (4\text{-}6)$$

where c_i is the concentration of the solute (mg/mL), V_i is the detector response (μV), t_i is the time (sec) at detector response V_i, and n is the number of data points. From equation (4-5), the dimensions of c_i and Δt_i in the numerator and denominator cancel out, and so μ has dimensions of time. Therefore V_i could be substituted for c_i in the estimation of μ. Similarly, σ^2 in equation (4-6) could also be estimated by using V_i instead of c_i .

The values of μ and σ^2 were corrected for the hold-up time and the dispersion in the tubing and the detector. Specifically, the terms μ' and $\sigma^{2\prime}$ were measured at five different flow rates (0.1-0.5 mL/min) with the column removed. These correction terms

were then subtracted directly from μ and σ^2 obtained from the experiments. Details are provided in Appendix B.

Chapter 5

Experimental Results

Sample response peaks at five different flow rates (0.1-0.5 mL/min) are illustrated in Figure 16 for glucose diffusion in silica gel-100. This Figure shows that at higher flow rates, the response peak eluents more quickly and the width of the peak narrows.

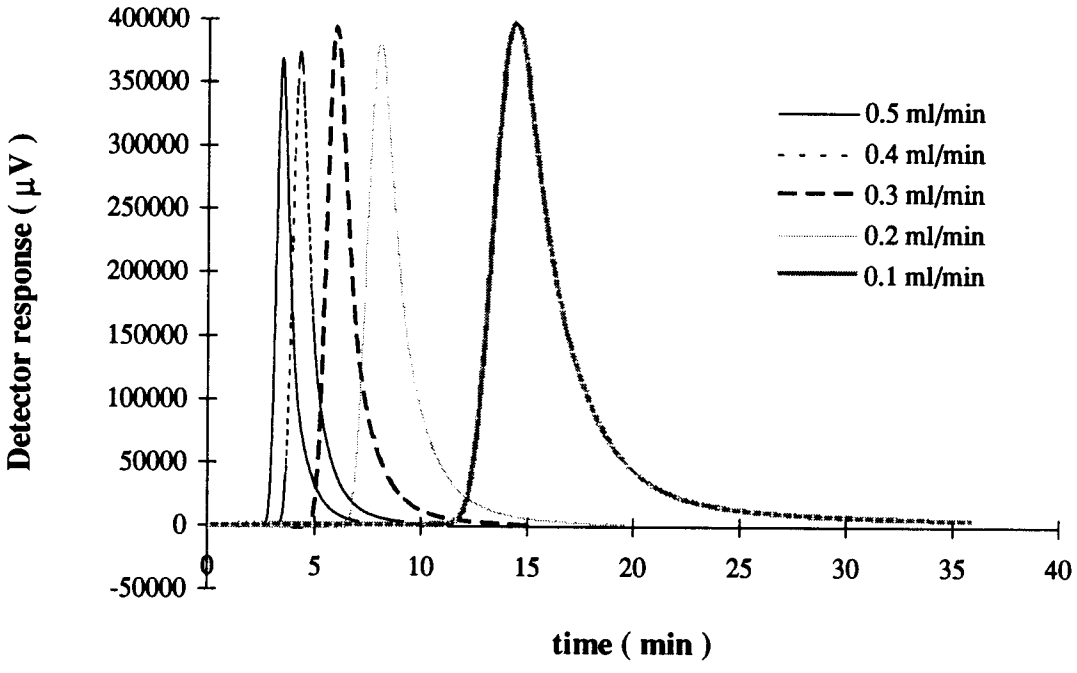

Figure 16. Response peaks of glucose diffusion in packed column of silica gel-100 catalyst (trial # 1).

The first moment (μ) and the second moment (σ^2) for each response peak were determined by equations (4-5) and (4-6) respectively. The HETP was calculated by

$$HETP = \frac{\sigma^2}{\mu^2} L \qquad (5\text{-}1)$$

Values for μ and HETP obtained by experiment for glucose and glucitol diffusion in each of the five catalysts are plotted as a function of interstitial velocity (U) in Figures 17 to 36. For each figure of μ vs.1/U (Figures 17-26), the data points represent values of μ calculated from the response peak while the solid line represents the value of μ obtained from the regression analysis. The intercept was forced to zero in the regression analysis.

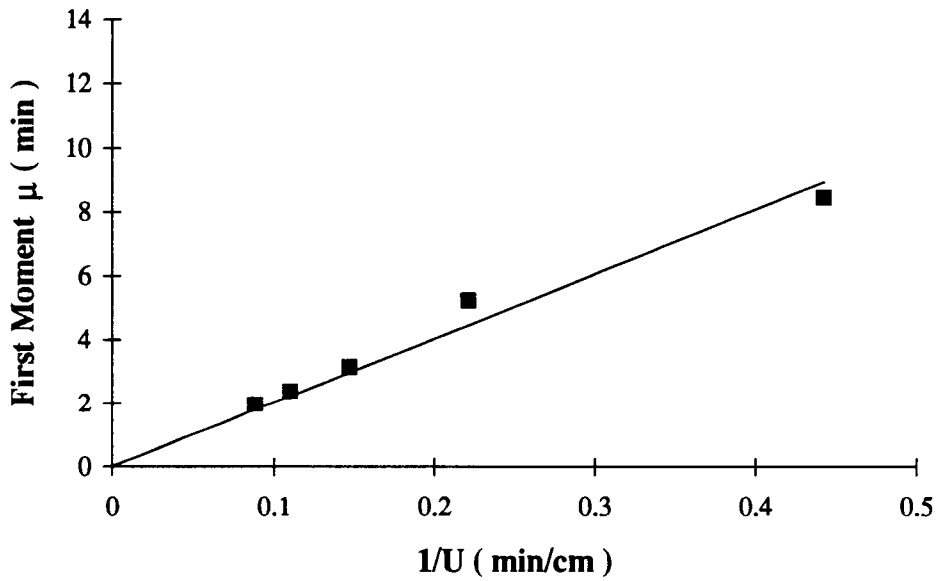

Figure 17. First moment of glucose diffusion in packed column of HY-zeolite catalyst (trial # 1).

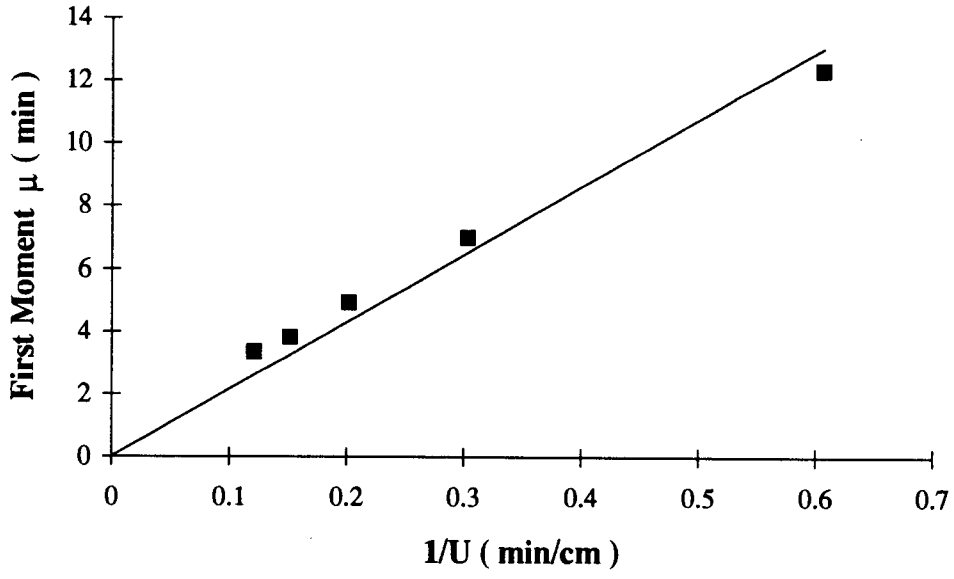

Figure 18. First moment of glucose diffusion in packed column of Na-MCM-20 catalyst (trial # 1).

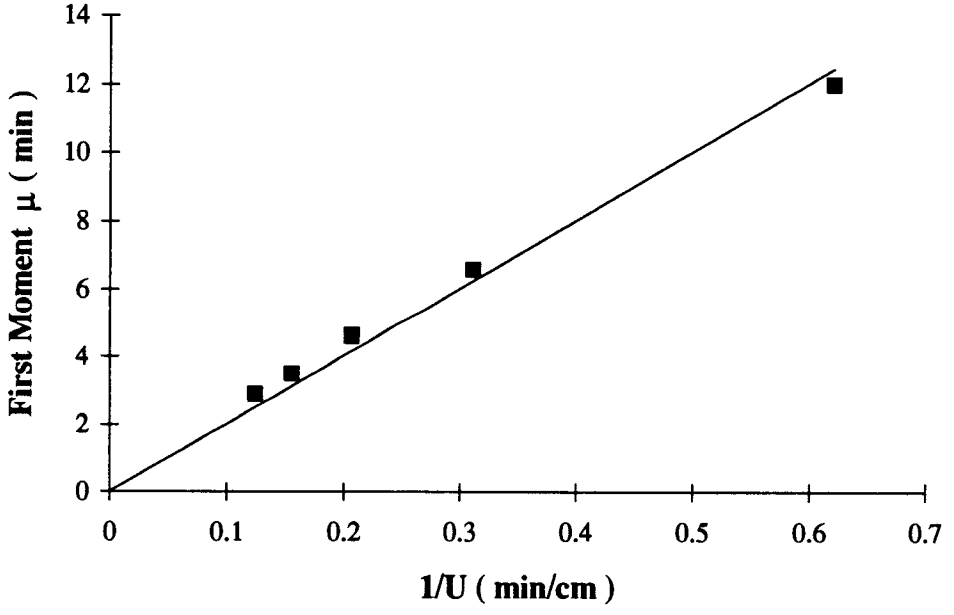

Figure 19. First Moment of glucose diffusion in packed column of Na-MCM-41 catalyst (trial # 1).

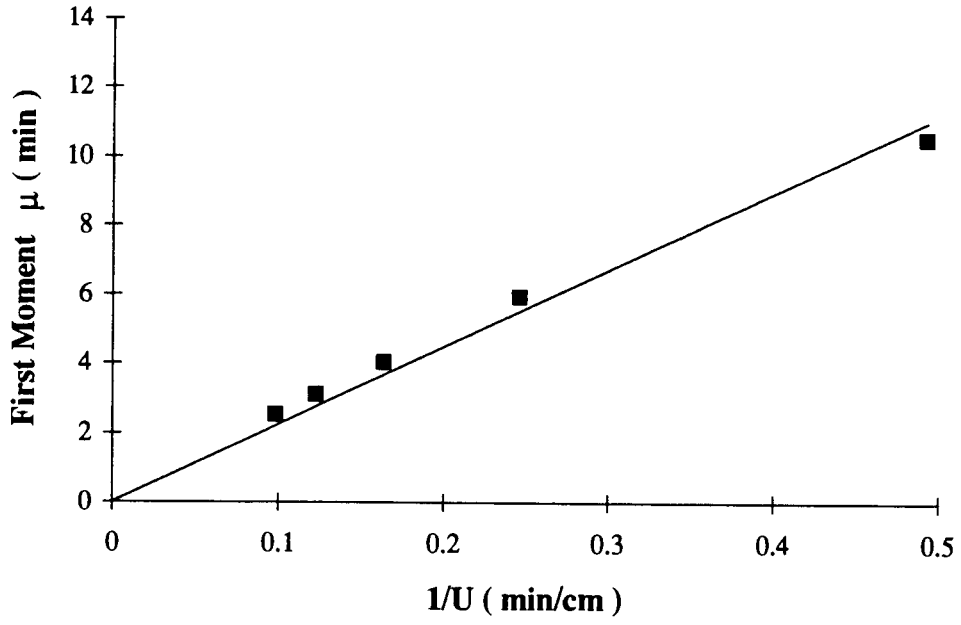

Figure 20. First moment of glucose diffusion in packed column of silica gel-60 catalyst (trial # 1).

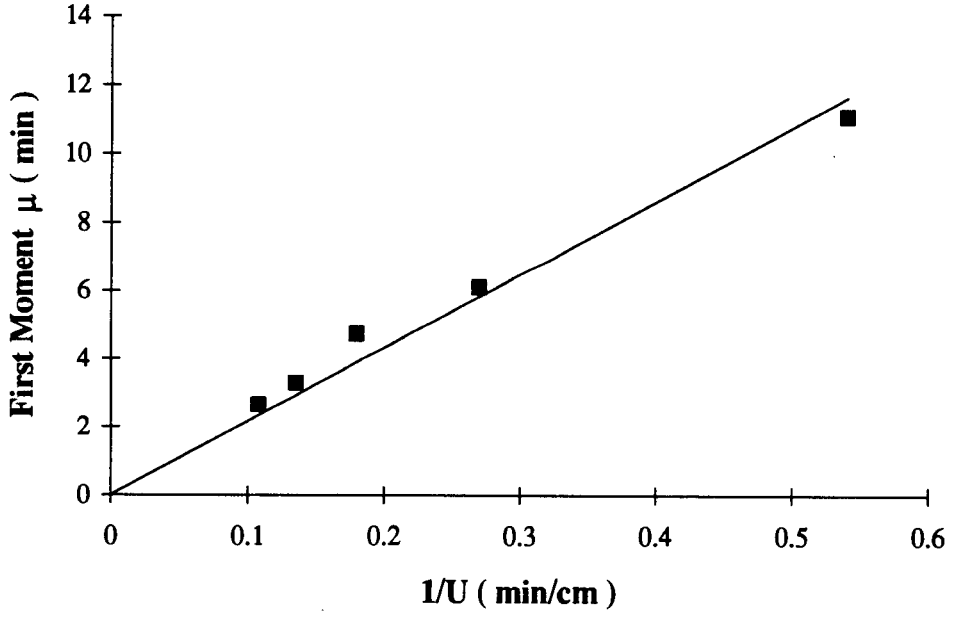

Figure 21. First moment of glucose diffusion in packed column of silica gel-100 catalyst (trial # 1).

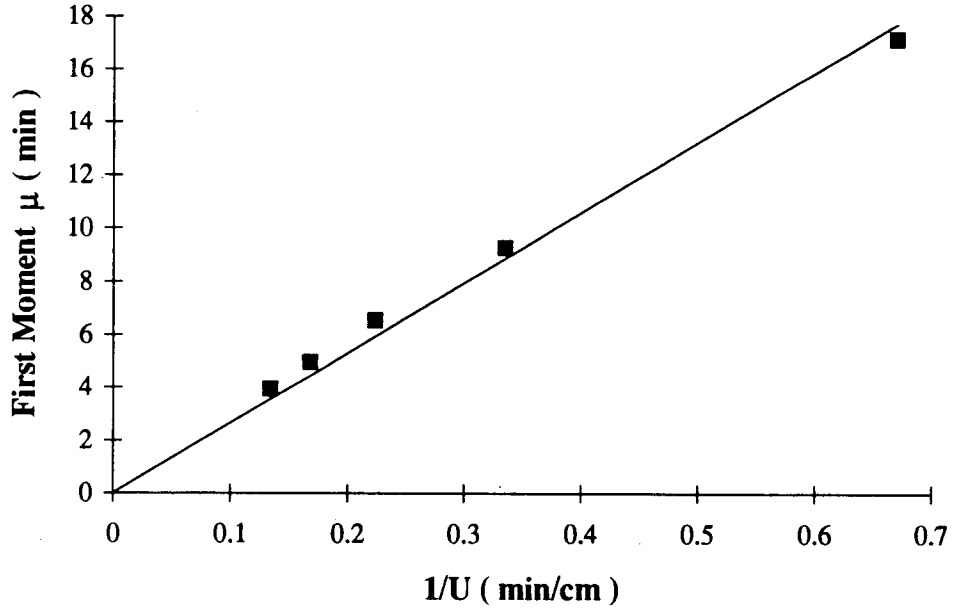

Figure 22. First moment of glucitol diffusion in packed column of HY-zeolite catalyst (trial # 1).

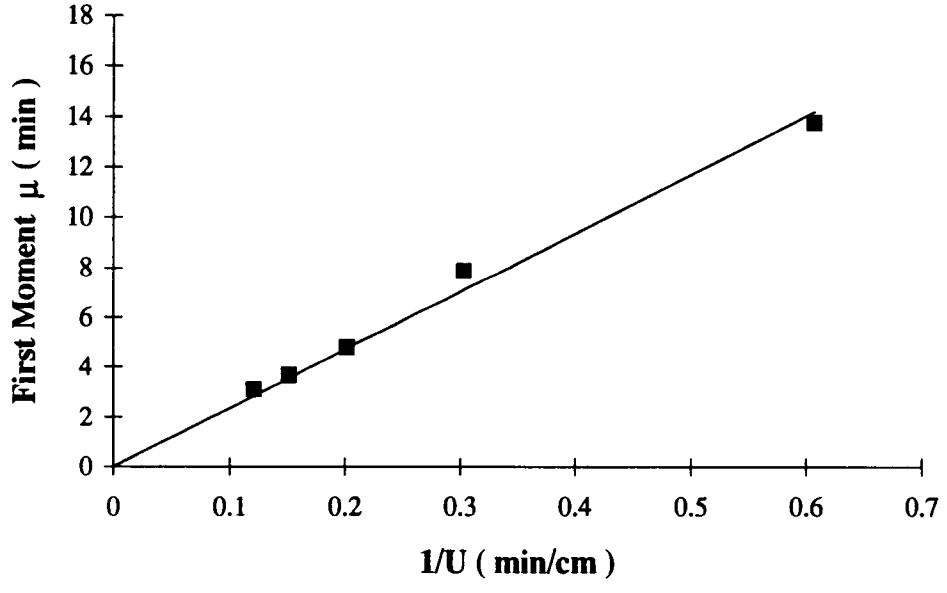

Figure 23. First moment of glucitol diffusion in packed column of Na-MCM-20 catalyst (trial # 1).

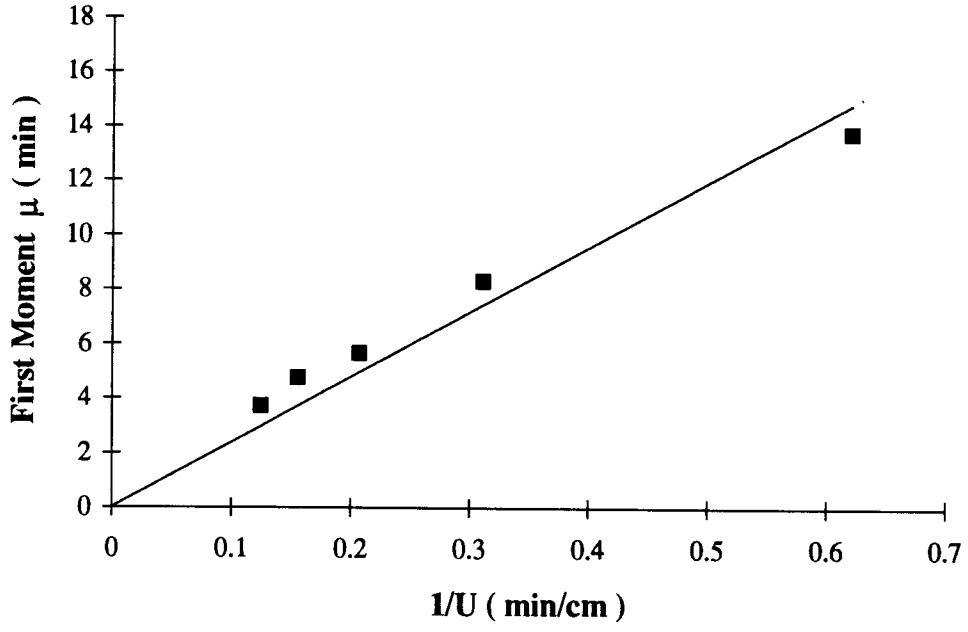

Figure 24. First moment of glucitol diffusion in packed column of Na-MCM-41 catalyst (trial # 1).

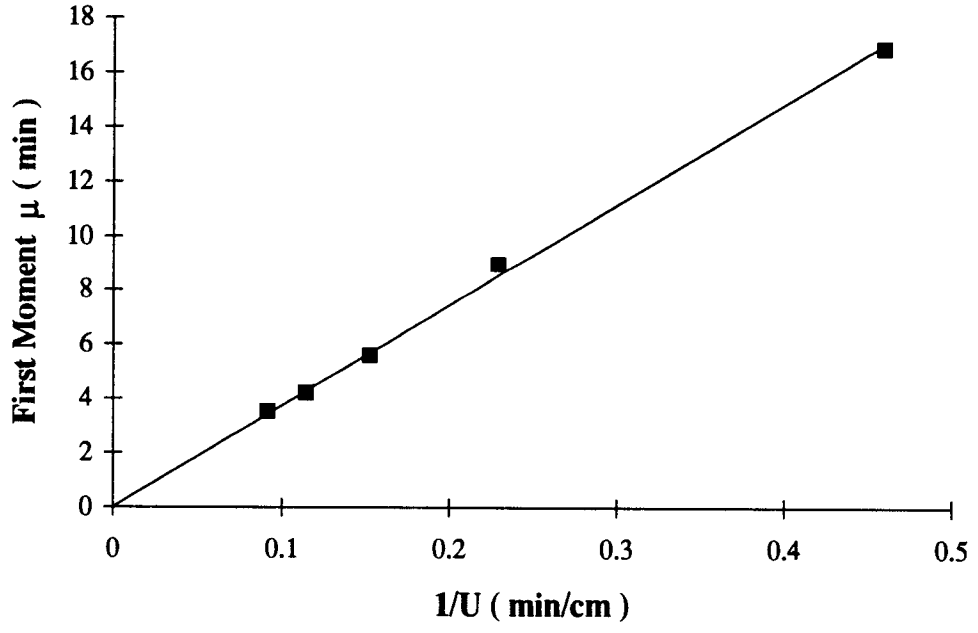

Figure 25. First moment of glucitol diffusion in packed column of silica gel-60 catalyst (trial # 1).

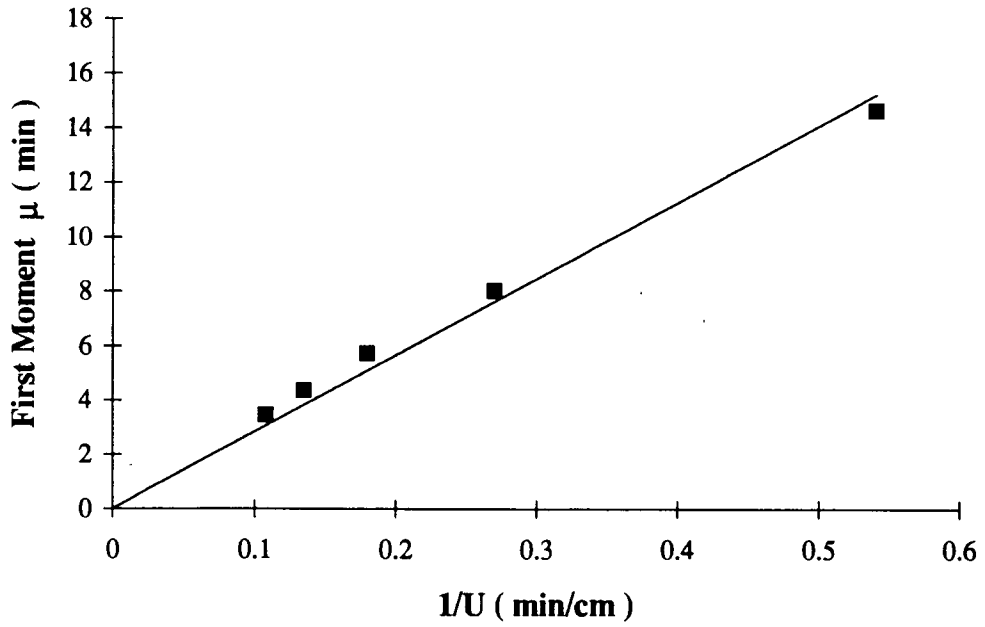

Figure 26. First moment of glucitol diffusion in packed column of silica gel-100 catalyst (trial # 1).

For each figure of HETP vs. U (Figures 27-36), the data points represent the value of HETP calculated from the response peak while the solid line represents the value of HETP obtained from the regression analysis. At very low flow rates ($U \rightarrow 0$), the term $2D_L/U$ in equation (3-15) dominates. Therefore, at very low flow rates, the value of HETP becomes larger and the intercept of HETP vs. U approaches infinity. The HPLC system in this study could not operate at very low flow rates (< 0.1 mL/min). The dotted line simply shows intercept from the regression analysis.

If we consider equations (3-16) to (3-20) as the limiting case at low Reynolds numbers, then the Peclet number (Pe) can be calculated from the intercept of HETP vs. U. The value of the Pe should be matched with the Pe estimated from equation (3-16). From equation (3-16), Pe depends only on the void fraction in the packed column. But in this study, the intercept depends on the characteristics of the packed column as well such as how uniformly the catalyst powder is packed. The intercepts for each column in this study were different depending on the characteristics of each column.

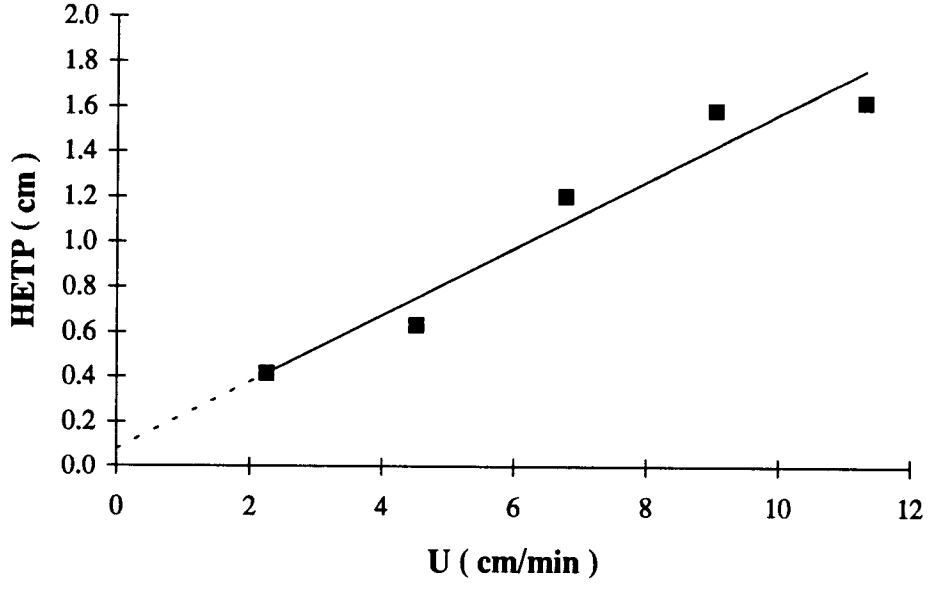

Figure 27. HETP of glucose diffusion in packed column of HY-zeolite catalyst (trial # 1).

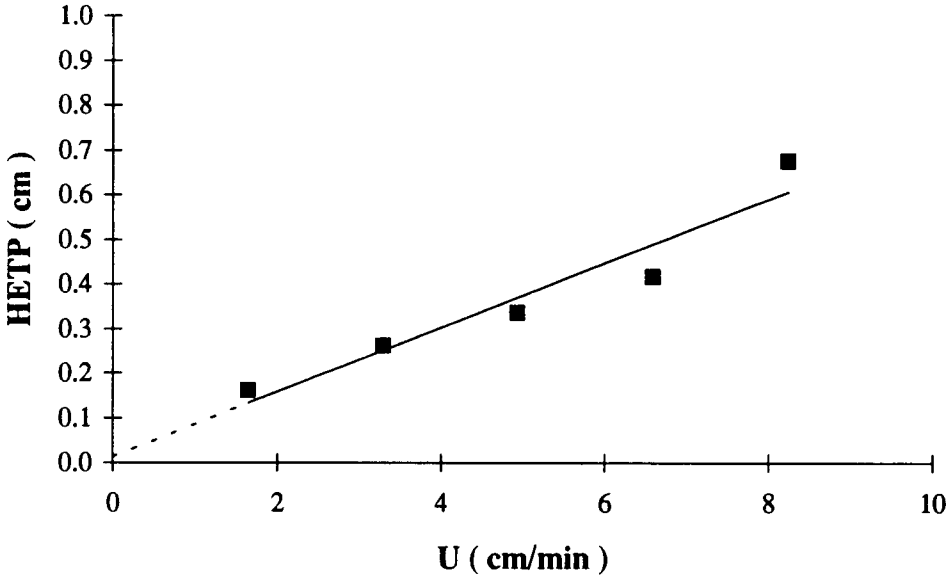

Figure 28. HETP of glucose diffusion in packed column of Na-MCM-20 catalyst (trial # 1).

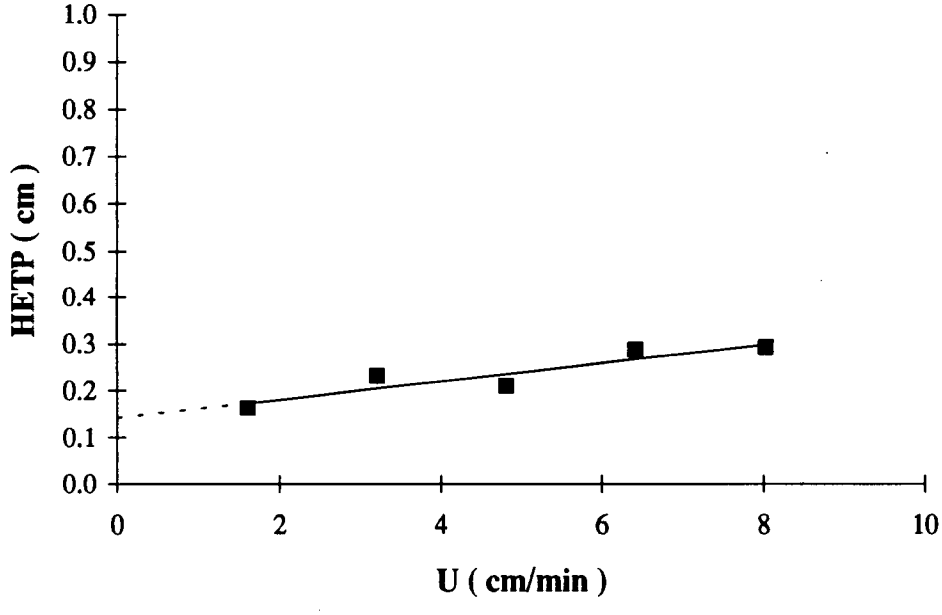

Figure 29. HETP of glucose diffusion in packed column of Na-MCM-41 catalyst (trial # 1).

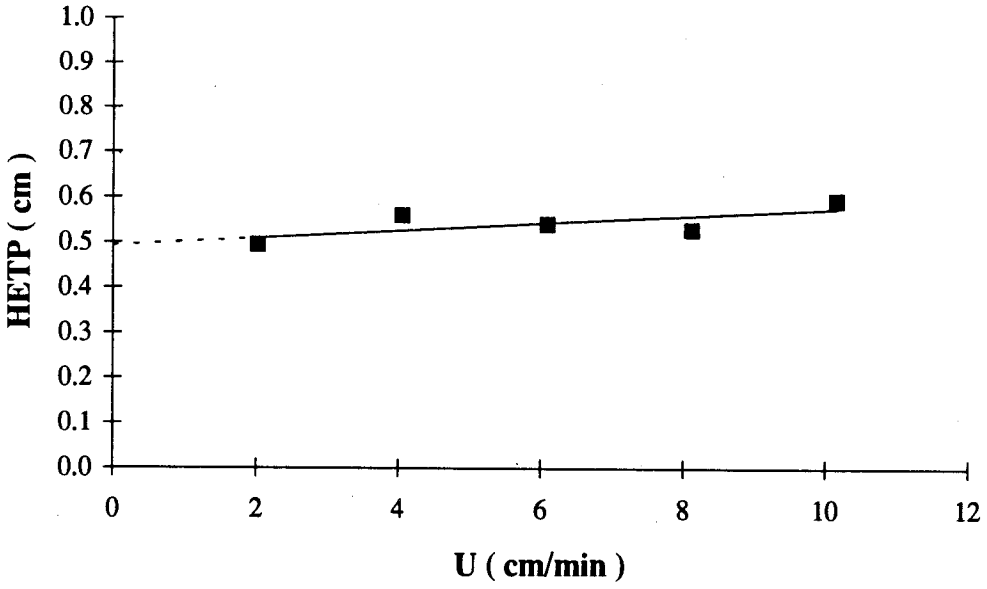

Figure 30. HETP of glucose diffusion in packed column of silica gel-60 catalyst (trial # 1).

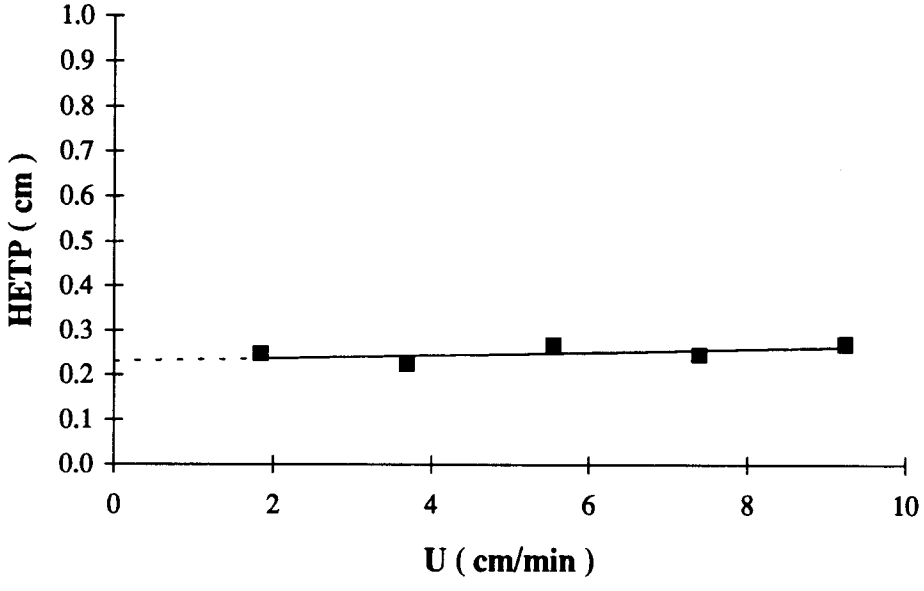

Figure 31. HETP of glucose diffusion in packed column of silica gel-100 catalyst (trial # 1).

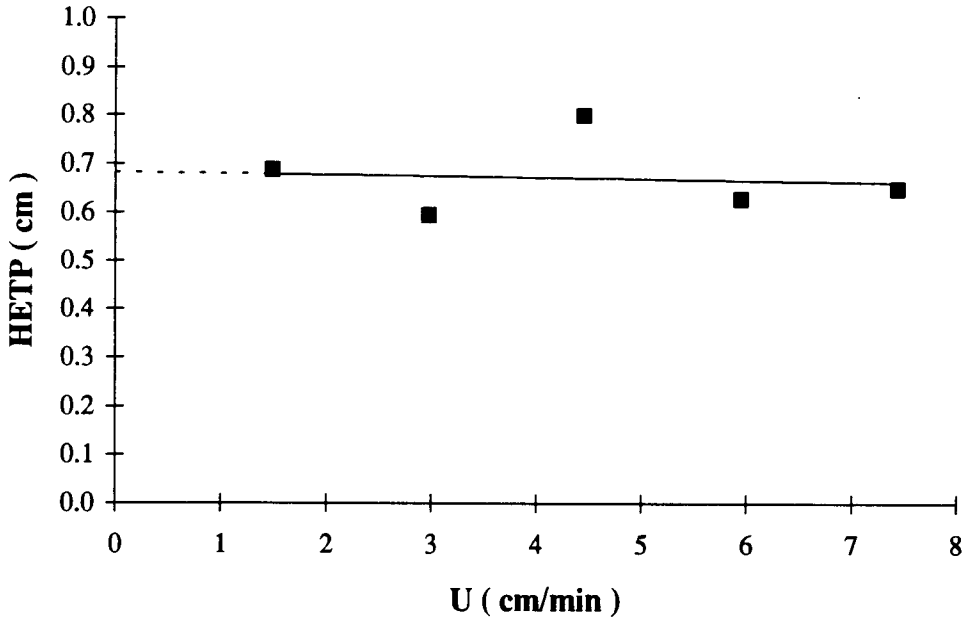

Figure 32. HETP of glucitol diffusion in packed column of HY-zeolite catalyst (trial # 1).

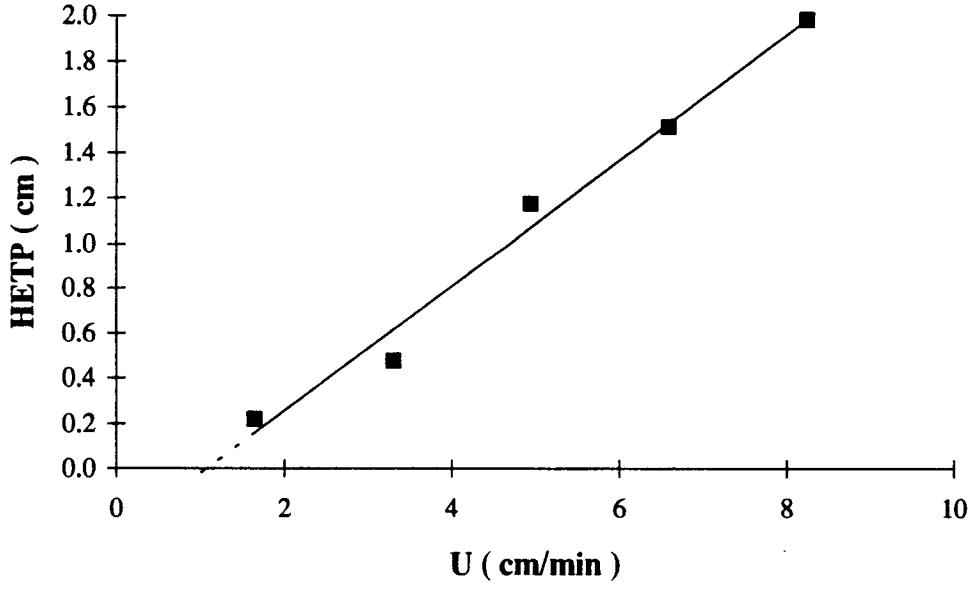

Figure 33. HETP of glucitol diffusion in packed column of Na-MCM-20 catalyst (trial # 1).

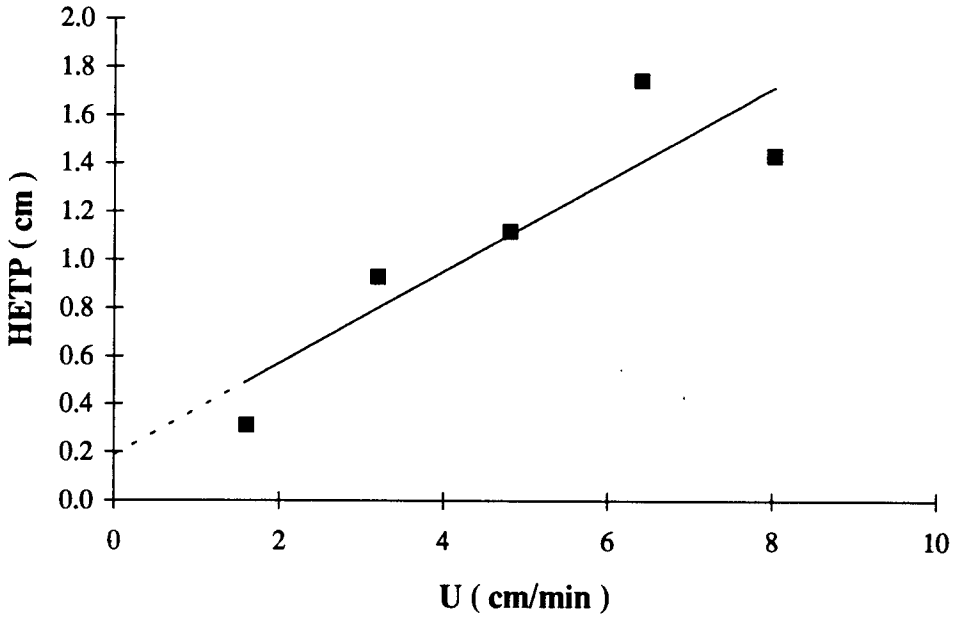

Figure 34. HETP of glucitol diffusion in packed column of Na-MCM-41 catalyst (trial # 1).

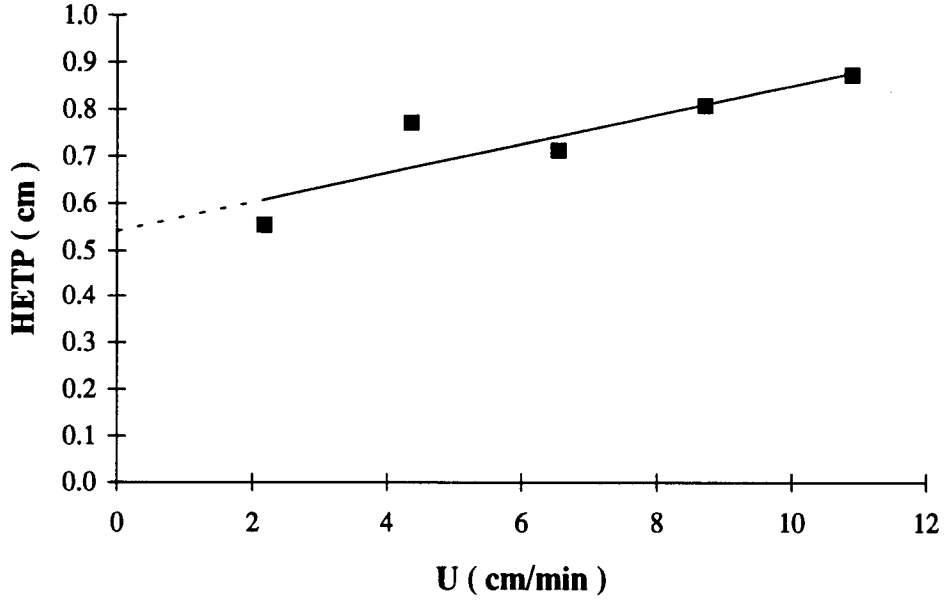

Figure 35. HETP of glucitol diffusion in packed column of silica gel-60 catalyst (trial # 1).

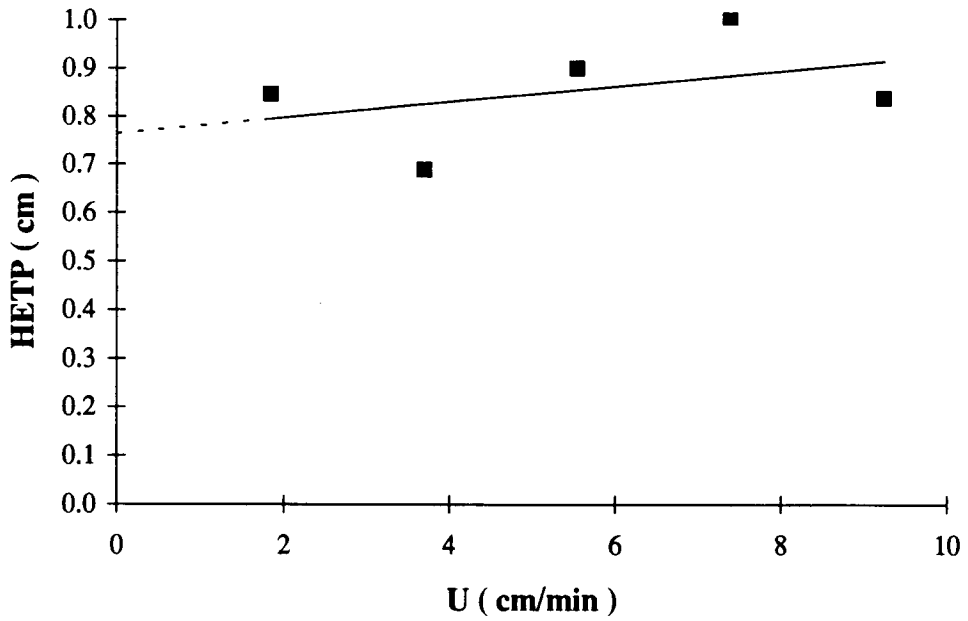

Figure 36. HETP of glucitol diffusion in packed column of silica gel-100 catalyst (trial # 1).

The adsorption equilibrium constant (K) was determined by the slope of μ vs. 1/U, and the intracrystalline diffusivity (D_c) was determined by the slope of HETP vs. U, as detailed in the Mathematical Analysis section. The results are shown in Table 6. The sample calculations are given in Appendix C, and data for each measurement are provided in Appendix D.

Table 6. Adsorption equilibrium constants (K) and intracrystalline diffusivities (D_c) of glucose and glucitol in the 5 catalysts.

Solute	Catalyst	Adsorption Equilibrium Constant, K (mL/mL)			Intracrystalline Diffusivity, D_C (cm^2/sec)		
		Trial # 1	Trial # 2	Average	Trial # 1	Trial # 2	Average
Glucose	HY-zeolite	0.379	0.381	0.380	1.78E-09	1.75E-09	1.77E-09
	Na-MCM-20	0.675	0.681	0.678	9.15E-09	8.91E-09	9.03E-09
	Na-MCM-41	0.619	0.624	0.622	1.77E-08	1.64E-08	1.71E-08
	silica gel-60	0.530	0.529	0.530	2.51E-07	2.49E-07	2.50E-07
	silica gel-100	0.571	0.584	0.578	1.04E-06	1.11E-06	1.08E-06
Glucitol	HY-zeolite	0.610	0.608	0.609	0.00E-00	0.00E-00	0.00E-00
	Na-MCM-20	0.789	0.782	0.786	2.62E-09	2.59E-09	2.61E-09
	Na-MCM-41	0.849	0.846	0.848	2.22E-09	2.14E-09	2.18E-09
	silica gel-60	1.17	1.18	1.18	7.81E-08	6.41E-08	7.11E-08
	silica gel-100	0.895	0.896	0.896	2.36E-07	2.22E-07	2.29E-07

As shown in Table 6, the results were very repeatable with standard errors generally less than 10 %.

For both glucose and glucitol, the values of K for Na-MCM-20 and Na-MCM-41 are comparable. The values of K for silica gel-60 and silica gel-100 are also comparable. The value of K for HY-zeolite is the lowest for both glucose and glucitol. When comparing the value of K between glucose and glucitol for each catalyst, K for glucose is lower than the K for glucitol. For both glucose and glucitol, D_c increases when the pore size of catalyst increases, and when comparing the value of D_c between glucose and glucitol for each catalyst, the D_c for glucose is higher than the D_c for glucitol.

Chapter 6

Discussion and Conclusions

The pore size of the catalyst has significant effect on the intracrystalline diffusivity (D_c) for both glucose and glucitol (Figure 37). The value for D_c increases when the pore size of the catalyst increases, because the solute can pass through the pore easier when the pore diameter is larger.

The intracrystalline diffusivity D_c of glucose is greater than that of glucitol, because the size and structure of the solute affects the ability of the solute to pass through the pores. The critical diameter is used to compare the difference in molecular size between glucose and glucitol. The critical diameter is the longest axis of the molecule, and is equal to 8.583 Å for glucose and 9.714 Å for glucitol (Table 1). Since glucitol has a larger critical diameter than glucose, its diffusion rate is more hindered through the pore, and thus has a lower diffusivity. However, the difference between the critical diameter of glucose and glucitol is very small only 1.131 Å. Therefore another molecular property needs to be considered, such as the molecular shape. From Figure 2, the glucose molecule approximates a sphere because the long and short axis are almost equal (8.583 Å and 8.417 Å respectively). Therefore the glucose molecule can fit in catalyst pores of 8.6 Å diameter and greater. However, glucitol (Figure 3) is a linear molecule of ellipsoidal shape, with width and length equal to 8.001 Å and 9.714 Å respectively. It is more difficult for glucitol to pass through 8.6 Å pore than glucose, because the glucitol molecule must orient its short axis (8.001 Å) to be in line with the 8.6 Å pore opening.

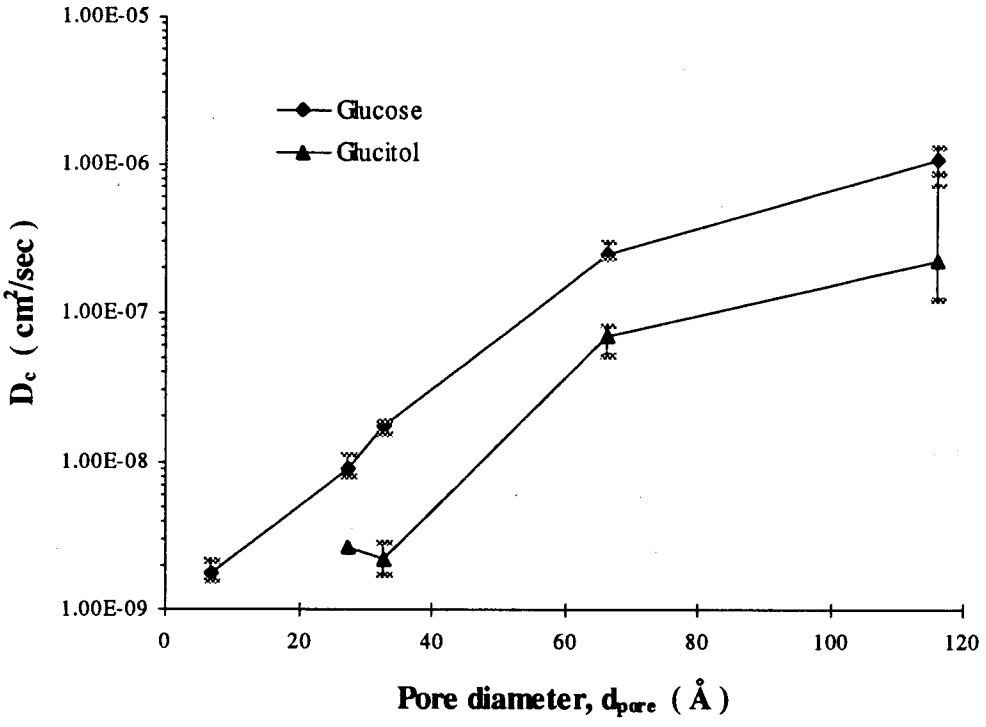

Figure 37. Effect of the pore size (d_{pore}) on the intracrystalline diffusivity (D_c).

When comparing the diffusion of glucose and glucitol in HY-zeolite, glucose was able to diffuse into HY-zeolite, but there was no diffusion of glucitol in HY-zeolite. From Figure 32, the slope of HETP vs.U for glucitol diffusion in a packed column of HY-zeolite catalyst is statistically zero. This means that the glucitol molecule is too large to penetrate into the pore of HY-zeolite. Therefore the intracrystalline diffusivity of glucitol in HY-zeolite is zero. Glucose has both a long axis and a short axis bigger than the 7.5 Å pore diameter of HY-zeolite but it still penetrates the pore of HY-zeolite, because D_c is finite. This result is difficult to understand. Perhaps the acidity of the HY-zeolite may open the cyclic ring of the glucose molecule to form a linear molecule which can pass through the pore. Alternatively, the glucose molecule could deform and become smaller in one

dimension when it interacts with the pore opening. However, this special case of diffusion will not be considered in the development of a model for predicting the D_e as a function of pore diameter.

The intracrystalline diffusivity of glucose and glucitol within the each of the five catalysts is less than the molecular diffusivity (D_m^0) of each solute in the solvent, even when the pore diameter of catalyst is as large as 100 Å. The value of D_m^0 for glucose in water at 30 ^{0}C is equal to 7.02×10^{-6} cm^2/sec (Chemical Engineers' Handbook, 1988). The value of D_m^0 for glucitol in water is estimated from the correlation proposed by Wilke and Chang (1955)

$$D_m^0 = \frac{7.4\times10^{-8} T(\Phi_f M_f)^{1/2}}{\mu_f V_f^{0.6}} \qquad (6\text{-}1)$$

where T is the absolute temperature (K), M_f is the molecular weight of the solvent, V_f is the molal volume of solute at the normal boiling point (cm^3/gmol), μ_f is the viscosity of the solvent (g/cm-sec), and Φ_f is the association parameter for the solvent. From equation (6-1), the value of D_m^0 for glucitol in water at 30 ^{0}C is equal to 7.65×10^{-6} cm^2/sec.

The intracrystalline diffusivity of a solute molecule in a catalyst pore is less than the molecular diffusivity of a solute in a solvent because of several effects, including the tortuosity effect, the concentration effect and the pore wall effect. An empirical model for

predicting the effective diffusivity (D_e) for nonadsorbed solutes proposed by Satterfield et al.(1973) is given by

$$\log_{10}(D_e / D_m^0) = -0.37 - 2.0\lambda \qquad (6\text{-}2)$$

where

$$\lambda = \frac{d_s}{d_{pore}} = \frac{r_s}{r_{pore}} \qquad (6\text{-}3)$$

In equation (6-3), the diameter of the solute (d_s) was taken as the longest axis of the molecule. Satterfield et al. suggested that the value of D_e / D_m^0 for a zero diameter solute, which is 0.43, should correspond to the reciprocal of the tortuosity ($\tau = 2.3$), and so equation (6-2) reduces to

$$\log_{10}(D_e \tau / D_m^0) = -2.0\lambda \qquad (6\text{-}4)$$

For this study, glucose and glucitol are also considered nonadsorbed solutes because the adsorption equilibrium constants for both glucose and glucitol are below 1 (Table 6). This implies that glucose and glucitol do not significantly adsorb on the catalysts shown in Table 6.

A plot of $\log_{10}(D_c / D_m^0)$ vs. λ for this study is shown in Figure 38.

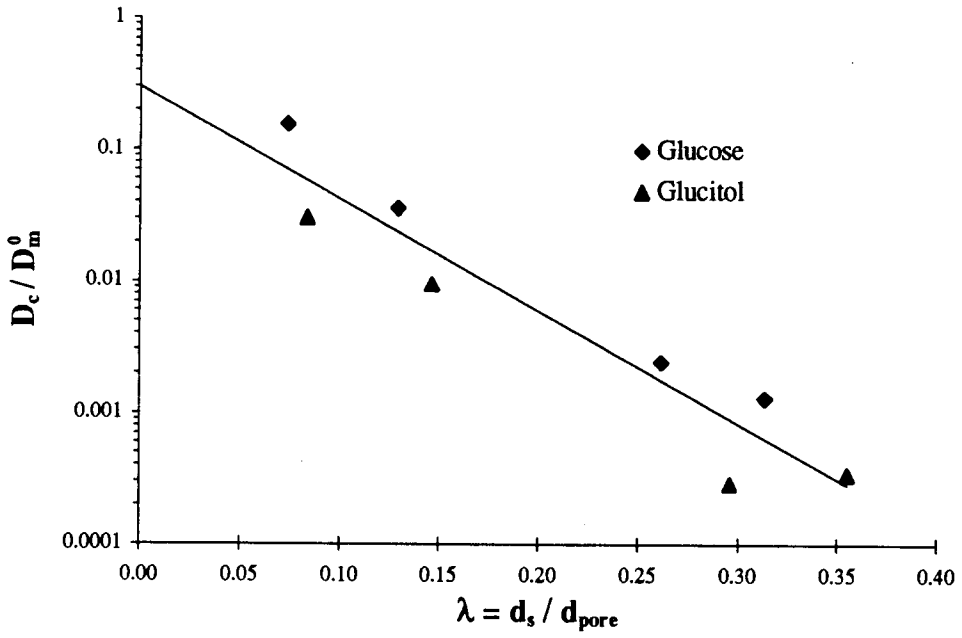

Figure 38. Effect of λ on the intracrystalline diffusivity (D_c).

The best straight line through the data is

$$\log_{10}(D_c / D_m^0) = -0.52 - 8.52\lambda \qquad (6\text{-}5)$$

Equation (6-5) shows that we also get an exponential dependence of D_c / D_m^0 on λ. But in this study five different catalysts were used, each with a separate tortuosity. Therefore the factor tortuosity could not be used to simplify equation (6-5) the same way as Satterfield et al. suggested in equation (6-4).

In general, the intracrystalline diffusivity can be correlated to the molecular diffusivity by

$$D_c = D_m^0 (F_1)(F_2) \qquad (6\text{-}6)$$

where F_1 and F_2 are corrections factors based on interactions of the solute and solvent molecules with the pore. In equation (6-6), Anderson and Quinn (1974) called F_1 the steric partition coefficient based on geometrical considerations. The solute molecules cannot occupy the region r_{pore} - r_s of the pore. In contrast, smaller solvent molecules can occupy this region. This effect decreases the concentration of the solute in the pore in comparison with its concentration immediately outside the pore in the bulk liquid. The cross sectional area of the pore available to the solute molecule divided by the total cross sectional area of the pore is the steric partitioning coefficient F_1. Mathematically, F_1 is defined as

$$F_1 = \frac{\pi (r_{pore} - r_s)^2}{\pi r_{pore}^2} = (1.0 - \lambda)^2 \qquad (6\text{-}7)$$

The correction factor F_2 in equation (6-6) proposed by Ternan (1987) accounts for the effect of the pore wall on the solvent. In principle, the force field from the pore wall could alter some of the factors which influence diffusivity in the bulk liquid. From equation (6-1), with the exception of solvent viscosity, all the terms are invariant physical properties of the solvent at isothermal conditions. Therefore the solvent viscosity is the only solution property which can be altered by the proximity of the pore wall. It is

hypothesized that a Van der Waals field force emanating from the pore wall will make the solvent near the wall more viscous than the solvent further away from the pore wall. An increase in viscosity would cause a decrease in diffusivity. By the analysis of Ternan, F_2 is defined as

$$F_2 = \frac{1}{1+P\lambda} \qquad (6\text{-}8)$$

where

$$P = [2-\lambda+\beta/\lambda(2-2\lambda-\beta)]\frac{\Delta\mu_w}{\mu_f} \qquad (6\text{-}9)$$

In equation (6-9), β is the ratio between the distance from the pore wall in which solvent has altered viscosity and the overall pore radius, and $\Delta\mu_w$ is the viscosity increment of solvent in the proximity of the pore wall (g/cm-sec). Equations (6-7) and (6-8) are substituted into equation (6-6) to obtain

$$\frac{D_c}{D_m^o} = \frac{(1-\lambda)^2}{1+P\lambda} \qquad (6\text{-}10)$$

A least squares estimate of the parameter P can be obtained by minimizing the sum of the squared residuals between D_c vs. λ data and equation (6-10). The best fit line is shown in Figure 39.

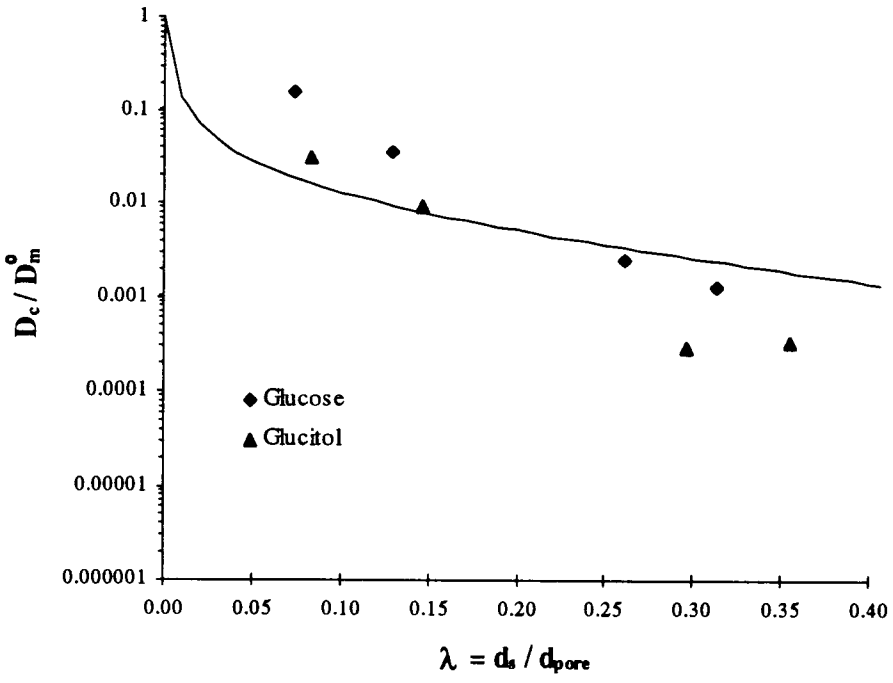

Figure 39. Diffusivity of solute vs. λ based on Ternan's model.

The solid line is the prediction based on equation (6-10) with P equal to 620. We can see that equation (6-10) represents the experimental data acceptably and has only one adjustable parameter. It also satisfies the two necessary limiting cases. First, it predicts D_c approaches zero when the diffusing solute molecule radius is equal to the pore radius ($\lambda \rightarrow 1$). Second, it predicts D_c approaches D_m^0 when the pore diameter is large compared with the diameter of the diffusing solute molecule ($\lambda \rightarrow 0$). Therefore this model can be used for predicting D_c with P equal to 620.

From this study, four conclusions can be deduced as shown below.

1) Glucose and glucitol are non-adsorbed solutes because their adsorption equilibrium constants (K) are below 1.

2) The intracrystalline diffusivity (D_c) of glucose and glucitol is significantly influenced by the pore diameter of the catalyst. For glucose, value of D_c increases from 1.77×10^{-9} to 1.08×10^{-6} cm^2/sec when the pore diameter of the catalyst increases from 7.5 Å to 100 Å.

3) The diffusivity of glucitol is two to four times lower than that of glucose over the 7.5 Å to 100 Å pore size range. Glucose and glucitol have almost the same molecular weight but have a significant difference in their diffusivities because of molecular size and structure effects. In particular, glucitol has a larger critical diameter than glucose, and so its diffusivity is lower. Furthermore, glucitol is an ellipsoidal-shaped molecule, and so has more difficulty passing through the pores than the spherical glucose molecule.

4) Two models reasonably predict the intracrystalline diffusivity of glucose and glucitol in microporous and mesoporous silica-based catalysts as a function of reduced pore diameter λ . The two models are

model 1 $$\log_{10}(D_c / D_m^0) = -0.52 - 8.52\lambda$$

model 2 $$\frac{D_c}{D_m^o} = \frac{(1-\lambda)^2}{1+620\lambda}$$

Model 2 is recommended because it has a fundamental basis and only one adjustable parameter.

Bibliography

Awum, F., S. Narayan, and D. Ruthven. 1988. Measurement of intracrystalline diffusivities in NaX zeolite by liquid chromatography. *Industrial and Engineering Chem. Res.* 27: 1510-1515.

Barrett, E.P., L.G. Joyner, and P.P. Halenda. 1951. The determination of pore volume and area distributions in porous substances I: computation from nitrogen isotherms. *Journal of American Chemical Society* 73: 373-380.

Beck, J.S., J.C. Vartuli, and W.J. Roth. 1992. A new family of mesoporous molecular sieves prepared with liquid crystal templates. *Journal of the American Chemical Society* 114: 10834-43.

Ching, C.B., H. Hidajat, and M.N. Rathor. 1989. Chromatographic evaluation of sorption and diffusion characteristics of glucose, maltose and maltotriose in silica gels. *Journal of Chromatography* 463: 261-270.

Haynes, H.W., and P.N. Sarma. 1973. A model for the application of gas chromatography to measurements of diffusion in bidisperse structured catalysts. *AICHE Journal* 19: 1043-1046.

Ho, C., C.B. Ching, and D.M. Ruthven. 1987. A comparative study of zeolite and resin adsorbents for the separation of fructose-glucose mixtures. *Industrial and Engineering Chem. Res.* 26: 1407-1412.

Horvath, G.E., and K. Kawazoe. 1983. Method for the calculation of effective pore size distribution in molecular sieve carbon. *Journal of Chemical Engineering of Japan* 16: 470-475.

Huber, K.P. 1972. *American Institute of Physics Handbook.* New York: McGraw-Hill.

Levenspiel, O. 1986. *Engineering Flow and Heat Exchange.* New York: Plenum Press.

Liley, P.E., R.C. Reid, and E. Buck. 1988. *Perry's Chemical Engineerings' Handbook.* Japan: Kosaido Printing Co., Ltd.

Lin, Y.S., and Y.H. Ma. 1989. A comparative chromatographic study of liquid adsorption and diffusion in microporous and macroporous adsorbents. *Industrial and Engineering Chem. Res.* 28: 622-630.

Lourvanij, K., and G.L. Rorrer. 1993. Reaction of Aqueous Glucose Solutions over Solid-Acid Y-Zeolite Catalyst at 110-160 ^{0}C. *Industrial and Engineering Chem. Res.* 32: 11-19.

Lourvanij, K., and G.L. Rorrer. 1994. Dehydration of glucose to organic acids in microporous pillared clay catalysts. *Applied Catalysis A: General* 109: 147-165.

Ma, Y.H., and Y.S. Lin. 1987. Adsorption and diffusion of liquids in silicalite using HPLC. *AICHE Symposium Series*. 83: 1-10.

Ma, Y.H., and Y.S. Lin. 1988. Adsorption and diffusion of polar and non-polar liquids in aluminas by HPLC. *AICHE Symposium Series*. 84: 1-12.

Satterfield, C. N., C.K. Colton, and W.H. Pitcher, JR. 1973. Restricted diffusion in liquids within fine pores. *AICHE Journal*. 19: 628-635.

Ternan, M. 1987. The diffusion of liquids in pores. *The Canadian Journal of Chemical Engineering*. 65: 244-249.

Uddin, M.S., K. Hidajat, and Chi-Bun Ching. 1990. Liquid chromatographic evaluation of equilibrium and kinetic parameters of large molecule amino acids on silica gel. *Industrial and Engineering Chem. Res.* 29: 647-651.

van der Laan, E.R. 1958. Letters to the editors: notes on the diffusion-type model for the longitudinal mixing in flow (O. Levenspiel and W.K. Smith). *Chem. Eng. Sci.* 7: 187-191.

Weast, R.C. 1979. *CRC Handbook of Chemistry and Physics*. Florida: CRC Press.

Wen, C.Y., and L.T. Fan. 1975. *Models for Flow Systems and Chemical Reactors*. Marcel Dekker.

Wilson, E.J., and C.J. Geankoplis. 1966. Liquid mass transfer at very low Reynolds numbers in packed beds. *Industrial and Engineering Chem. Fund.* 5:9-14.

Appendices

Appendix A: Determination of Molecular Dimensions

Atom	Van der waals Radii [a]	Atomic Radii [b]
H	1.2 Å	0.74138 Å
O	1.4 Å	1.20750 Å

(a) *CRC Handbook of Chemistry & Physics*, 59th Edition, p.D-230 (1979)

(b) *American Institute of Physics Handbook*, New York, p.175,179 (1972)

Glucose

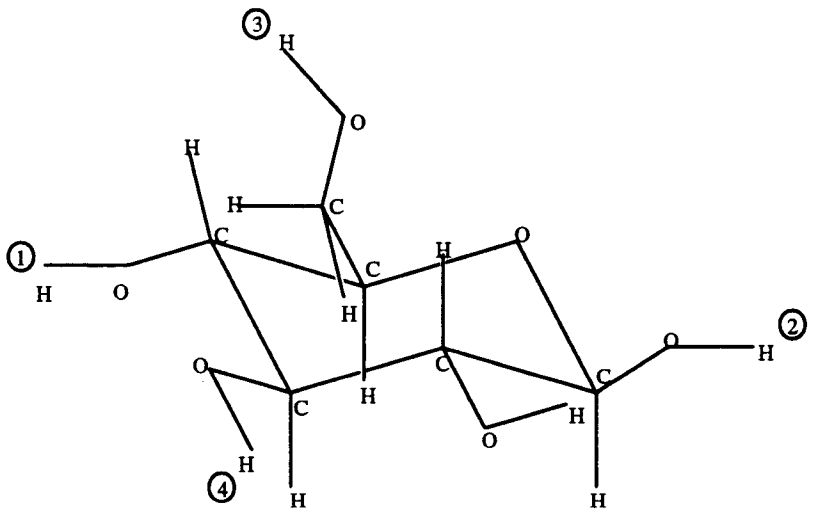

The length between (1) and (2) is equal to 6.01724 Å, and the length between (3) and (4) is equal to 6.18282 Å (calculated by Hyperchem Software). The longest short axis is the length between (1) and (2) including the radius of H, and the long axis is the length between (3) and (4) including the radius of H.

Longest short axis

Van der Waals Radii = 6.01724 + 2 (1.2) = 8.417 Å

Atomic Radii = 6.01724 + 2 (0.74138) = 7.5 Å

Long axis

Van der Waals Radii = 6.18282 + 2 (1.2) = 8.583 Å

Atomic Radii = 6.18282 + 2 (0.74138) = 7.665 Å

Glucitol

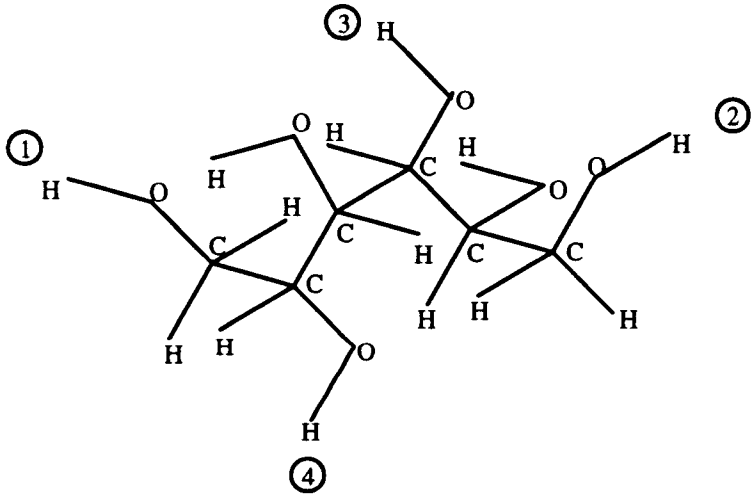

The length between (1) and (2) is equal to 7.31422 Å, and the length between (3) and (4) is equal to 5.60102 Å (calculated by Hyperchem Software). The long axis is the

length between (1) and (2) including the radius of H, and the longest short axis is the length between (3) and (4) including the radius of H.

Long axis

Van der Waals Radii = 7.31422 + 2 (1.2) = 9.714 Å

Atomic Radii = 7.31422 + 2 (0.74138) = 8.797 Å

Longest short axis

Van der Waals Radii = 5.60102 + 2 (1.2) = 8.001 Å

Atomic Radii = 5.60102 + 2 (0.74138) = 7.084 Å

Appendix B: Corrections for First Moment (μ) and Second Moment (σ^2)

The RI detector and the tubing in the HPLC system used in this study have a dead volume. Therefore, it is very important to correct for the effect of dead volume on the response peak. To correct for the effect of dead volume, the delay time of the blank response peak μ' with the column removed is simply subtracted from the first moment (μ) obtained from the experiment. The variance of the blank response peak $\sigma^{2'}$ with the column removed is subtracted directly from the second moment (σ^2) obtained from the experiment to find the second moment attributable to the column itself. The correction equations are given below:

$$\underset{\text{(corrected first moment)}}{\mu} = \underset{\text{(raw first moment)}}{\mu} - \underset{\text{(delay time of the blank peak)}}{\mu'} \qquad \text{(B-1)}$$

$$\underset{\text{(corrected second moment)}}{\sigma^2} = \underset{\text{(raw second moment)}}{\sigma^2} - \underset{\text{(variance of the blank peak)}}{\sigma^{2'}} \qquad \text{(B-2)}$$

The corrections of the first Moment (μ) and Second Moment (σ^2) are summarized in Table B-1.

Table B-1. Example for the corrections of μ and σ^2 of glucose diffusion in packed column of HY-zeolite catalyst (trial # 1).

Flow rate (mL/min)	Uncorrected First Moment (min)	Delay time of Blank Peak (min)	Corrected First Moment (min)	Uncorrected Second Moment (min^2)	Variance of Blank Peak (min^2)	Corrected Second Moment (min^2)
0.1	13.52	5.069	8.453	8.844	5.879	2.965
0.2	8.024	2.781	5.243	3.535	1.805	1.730
0.3	5.072	1.926	3.145	2.092	0.899	1.193
0.4	3.872	1.499	2.374	1.484	0.589	0.894
0.5	3.145	1.192	1.953	0.993	0.374	0.619

The corrected first moment (μ) and the corrected second moment (σ^2) will be used for the determinations of K and D_c in this study.

Appendix C: Determination of Adsorption Equilibrium Constant (K) and Intracrystalline Diffusivity (D_c)

The adsorption equilibrium constant (K) is determined directly by the slope of μ vs. 1/U using equation (3-13) as demonstrated in example C-1.

Example C-1

Determination of K for glucose diffusion in packed column of HY-zeolite (trial # 1).

Length of the packing (L) = 10 cm

Void fraction in packed bed (ε) = 0.27 mL/mL

Slope of μ vs. 1/U from regression analysis = 20.24 cm

From equation (3-13), μ is equal to $\frac{L}{U}\left[1+\frac{(1-\varepsilon)}{\varepsilon}K\right]$ and the slope of μ vs. 1/U is equal to $L\left[1+\frac{(1-\varepsilon)}{\varepsilon}K\right]$.

$$\text{Slope} = L\left[1+\frac{(1-\varepsilon)}{\varepsilon}K\right]$$

$$20.24 = 10\ (\ 1+(\ 1\text{-}0.27\ )K/0.27\ )$$

$$K = 0.38\ \text{mL/mL}$$

The intracrystalline diffusivity (D_c) is obtained directly from the slope of HETP vs. U in the linear region using equation (3-15) as demonstrated in example C-2.

Example C-2

Determination of D_c for glucose diffusion in packed column of HY-zeolite (trial # 1).

Density of the solvent (ρ_f) at 30 ^{0}C = 998.2 kg/m^3

Viscosity of the solvent (μ_f) at 30 ^{0}C = 993×10^{-6} kg/m-sec

Particle diameter (d_p) = 23.71 μ m

Particle porosity (ε_p) = 0.25 mL/mL

Void fraction in packed bed (ε) = 0.27 mL/mL

Molecular diffusivity (D_m^0) of glucose in water at 30 ^{0}C = 7.02×10^{-6} cm^2/sec

Adsorption equilibrium constant (K) = 0.38 mL/mL

Slope of HETP vs.U from regression analysis (B) = 0.15 min

Reynolds number (Re)

From equation (3-23),

$$Re = \frac{\rho_f \varepsilon U d_p}{\mu_f} \qquad (C\text{-}1)$$

For lowest velocity, U = 2.26 cm/min, Re = 0.0024

For highest velocity, U = 11.3 cm/min, Re = 0.012

The results show that Re are in the range of 0.0015-55, so the correlation for the Sherwood number in equation (3-21) is valid.

External film mass transfer coefficient (k_f)

From equations (3-21) to (3-24),

$$k_f = 1.09\left(\frac{D_m^0}{d_p \varepsilon}\right)^{0.67} U^{0.33} \qquad \text{(C-2)}$$

The average interstitial velocity ($\overline{U}$) is used in this calculation (as stated in chapter 3), and the value is calculated from the average of the lowest and highest values for U: $\overline{U}$ = (2.26 + 11.3) / 5 = 6.78 cm/min. Substitution of D_m^0 , d_p, ε , and U into equation (C-2) gives k_f = 1.55 cm/min.

From equation (3-15), the slope is

$$B = 2\left(\frac{\varepsilon}{1-\varepsilon}\right)\left\{\frac{R_p}{3k_f} + \frac{R_p^2(K-\varepsilon_p)}{15K^2 D_c}\right\}\left\{1+\frac{\varepsilon}{(1-\varepsilon)K}\right\}^{-2} \qquad \text{(C-3)}$$

By substituting the slope, R_p, k_f, K, ε_p and ε into equation (C-3), the intracrystalline diffusivity (D_c) is calculated by the computer and it is equal to 1.78×10^{-9} cm^2/sec.

Appendix D: Experimental Data for Diffusivity Estimation

Table D-1. Glucose diffusion in packed column of HY-zeolite catalyst (trial # 1).

1/Interstitial velocity,	Corrected first moment,	Regression Statistics			
1/U	μ				
(min/cm)	(min)	Multiple R	0.984		
		R Square	0.968		
0.442	8.453	Adjusted R Square	0.718		
0.221	5.243	Standard Error	0.476		
0.147	3.145	Observations	5		
0.111	2.374				
0.088	1.953		Coefficients	Standard Error	t Statistic
		Intercept	0	#N/A	#N/A
		x1	20.239	0.890	22.745
Interstitial velocity,	Corrected first moment,	Corrected second moment,	HETP		
U	μ	σ^2			
(cm/min)	(min)	$(\text{min})^2$	(cm)		
2.26	8.453	2.965	0.415		
4.52	5.243	1.730	0.629		
6.78	3.145	1.193	1.206		
9.04	2.374	0.894	1.588		
11.30	1.953	0.619	1.623		
Regression Statistics					
Multiple R	0.969				
R Square	0.939				
Adjusted R Square	0.918				
Standard Error	0.157				
Observations	5				
	Coefficients	Standard Error	t Statistic		
Intercept	0.080	0.165	0.482		
x1	0.149	0.022	6.783		

Table D-2. Glucose diffusion in packed column of HY-zeolite catalyst (trial # 2).

1/Interstitial velocity,	Corrected first moment,	Regression Statistics			
1/U	μ				
(min/cm)	(min)	Multiple R	0.986		
		R Square	0.973		
0.442	8.544	Adjusted R Square	0.723		
0.221	5.258	Standard Error	0.451		
0.147	3.069	Observations	5		
0.111	2.262				
0.088	1.964		Coefficients	Standard Error	t Statistic
		Intercept	0	#N/A	#N/A
		x1	20.311	0.843	24.098
Interstitial velocity,	Corrected first moment,	Corrected second moment,	HETP		
U	μ	σ^2			
(cm/min)	(min)	$(min)^2$	(cm)		
2.26	8.544	3.023	0.414		
4.52	5.258	1.866	0.675		
6.78	3.069	1.197	1.272		
9.04	2.262	0.921	1.800		
11.30	1.964	0.613	1.590		
Regression Statistics					
Multiple R	0.930				
R Square	0.865				
Adjusted R Square	0.819				
Standard Error	0.251				
Observations	5				
	Coefficients	Standard Error	t Statistic		
Intercept	0.107	0.263	0.407		
x1	0.154	0.035	4.377		

Table D-3. Glucose diffusion in packed column of Na-MCM-20 catalyst (trial # 1).

1/Interstitial velocity,	Corrected first moment,	Regression Statistics			
1/U	μ				
(min/cm)	(min)	Multiple R	0.982		
		R Square	0.965		
0.607	12.341	Adjusted R Square	0.715		
0.303	6.988	Standard Error	0.685		
0.202	4.911	Observations	5		
0.152	3.817				
0.121	3.344		Coefficients	Standard Error	t Statistic
		Intercept	0	#N/A	#N/A
		x1	21.501	0.933	23.038
Interstitial velocity,	Corrected first moment,	Corrected second moment,	HETP		
U	μ	σ^2			
(cm/min)	(min)	$(\text{min})^2$	(cm)		
1.65	12.341	2.442	0.160		
3.30	6.988	1.272	0.260		
4.94	4.911	0.807	0.335		
6.59	3.817	0.606	0.416		
8.24	3.344	0.757	0.677		
Regression Statistics					
Multiple R	0.960				
R Square	0.921				
Adjusted R Square	0.894				
Standard Error	0.064				
Observations	5				
	Coefficients	Standard Error	t Statistic		
Intercept	0.013	0.067	0.191		
x1	0.072	0.012	5.907		

Table D-4. Glucose diffusion in packed column of Na-MCM-20 catalyst (trial # 2).

1/Interstitial velocity,	Corrected first moment,	Regression Statistics			
1/U	μ				
(min/cm)	(min)	Multiple R	0.981		
		R Square	0.963		
0.607	12.383	Adjusted R Square	0.713		
0.303	7.030	Standard Error	0.707		
0.202	4.923	Observations	5		
0.152	3.847				
0.121	3.407		Coefficients	Standard Error	t Statistic
		Intercept	0	#N/A	#N/A
		x1	21.598	0.963	22.420
Interstitial velocity,	Corrected first moment,	Corrected second moment,	HETP		
U	μ	σ^2			
(cm/min)	(min)	$(\text{min})^2$	(cm)		
1.65	12.383	2.612	0.170		
3.3	7.030	1.676	0.339		
4.94	4.923	0.884	0.365		
6.59	3.847	0.499	0.337		
8.24	3.407	0.911	0.785		
Regression Statistics					
Multiple R	0.847				
R Square	0.718				
Adjusted R Square	0.624				
Standard Error	0.140				
Observations	5				
	Coefficients	Standard Error	t Statistic		
Intercept	0.031	0.147	0.209		
x1	0.075	0.027	2.764		

Table D-5. Glucose diffusion in packed column of Na-MCM-41 catalyst (trial # 1).

1/Interstitial velocity,	Corrected first moment,	Regression Statistics			
1/U	μ				
(min/cm)	(min)	Multiple R	0.993		
		R Square	0.985		
0.621	12.013	Adjusted R Square	0.735		
0.312	6.590	Standard Error	0.445		
0.207	4.601	Observations	5		
0.156	3.496				
0.125	2.883		Coefficients	Standard Error	t Statistic
		Intercept	0	#N/A	#N/A
		x1	20.105	0.592	33.946
Interstitial velocity,	Corrected first moment,	Corrected second moment,	HETP		
U	μ	σ^2			
(cm/min)	(min)	$(min)^2$	(cm)		
1.61	12.013	2.338	0.162		
3.21	6.590	1.001	0.230		
4.82	4.601	0.444	0.210		
6.42	3.496	0.350	0.287		
8.03	2.883	0.242	0.291		
Regression Statistics					
Multiple R	0.915				
R Square	0.838				
Adjusted R Square	0.784				
Standard Error	0.025				
Observations	5				
	Coefficients	Standard Error	t Statistic		
Intercept	0.141	0.027	5.331		
x1	0.020	0.005	3.937		

Table D-6. Glucose diffusion in packed column of Na-MCM-41 catalyst (trial # 2).

1/Interstitial velocity,	Corrected first moment,	Regression Statistics			
1/U	μ				
(min/cm)	(min)	Multiple R	0.993		
		R Square	0.985		
0.621	12.058	Adjusted R Square	0.735		
0.312	6.610	Standard Error	0.447		
0.207	4.632	Observations	5		
0.156	3.478				
0.125	2.908		Coefficients	Standard Error	t Statistic
		Intercept	0	#N/A	#N/A
		x1	20.178	0.594	33.982
Interstitial velocity,	Corrected first moment,	Corrected second moment,	HETP		
U	μ	σ^2			
(cm/min)	(min)	$(min)^2$	(cm)		
1.61	12.058	2.490	0.171		
3.21	6.610	0.911	0.209		
4.82	4.632	0.497	0.232		
6.42	3.478	0.345	0.285		
8.03	2.908	0.257	0.304		
Regression Statistics					
Multiple R	0.990				
R Square	0.981				
Adjusted R Square	0.974				
Standard Error	0.009				
Observations	5				
	Coefficients	Standard Error	t Statistic		
Intercept	0.137	0.009	15.009		
x1	0.021	0.002	12.398		

Table D-7. Glucose diffusion in packed column of silica gel-60 catalyst (trial # 1).

1/Interstitial velocity,	Corrected first moment,	Regression Statistics			
1/U	μ				
(min/cm)	(min)	Multiple R	0.991		
		R Square	0.982		
0.493	10.538	Adjusted R Square	0.732		
0.246	5.926	Standard Error	0.435		
0.164	4.032	Observations	5		
0.123	3.097				
0.098	2.517		Coefficients	Standard Error	t Statistic
		Intercept	0	#N/A	#N/A
		x1	22.366	0.730	30.634
Interstitial velocity,	Corrected first moment,	Corrected second moment,	HETP		
U	μ	σ^2			
(cm/min)	(min)	$(min)^2$	(cm)		
2.03	10.538	5.490	0.494		
4.06	5.926	1.966	0.560		
6.10	4.032	0.878	0.540		
8.13	3.097	0.508	0.529		
10.16	2.517	0.377	0.595		
Regression Statistics					
Multiple R	0.722				
R Square	0.521				
Adjusted R Square	0.362				
Standard Error	0.030				
Observations	5				
	Coefficients	Standard Error	t Statistic		
Intercept	0.493	0.031	15.799		
x1	0.008	0.005	1.808		

Table D-8. Glucose diffusion in packed column of silica gel-60 catalyst (trial # 2).

1/Interstitial velocity,	Corrected first moment,	Regression Statistics			
1/U	μ				
(min/cm)	(min)	Multiple R	0.991		
		R Square	0.983		
0.493	10.541	Adjusted R Square	0.733		
0.246	5.917	Standard Error	0.425		
0.164	3.981	Observations	5		
0.123	3.112				
0.098	2.519		Coefficients	Standard Error	t Statistic
		Intercept	0	#N/A	#N/A
		x1	22.346	0.714	31.312
Interstitial velocity,	Corrected first moment,	Corrected second moment,	HETP		
U	μ	σ^2			
(cm/min)	(min)	$(\text{min})^2$	(cm)		
2.03	10.541	5.462	0.492		
4.06	5.917	1.985	0.567		
6.10	3.981	0.790	0.499		
8.13	3.112	0.511	0.528		
10.16	2.519	0.379	0.597		
Regression Statistics					
Multiple R	0.600				
R Square	0.361				
Adjusted R Square	0.147				
Standard Error	0.042				
Observations	5				
	Coefficients	Standard Error	t Statistic		
Intercept	0.485	0.044	11.117		
x1	0.008	0.006	1.301		

Table D-9. Glucose diffusion in packed column of silica gel-60 catalyst (trial # 3).

1/Interstitial velocity,	Corrected first moment,	Interstitial velocity,	Corrected second moment,	HETP
1/U	μ	U	σ^2	
(min/cm)	(min)	(cm/min)	(min)^2	(cm)
0.493	10.356	2.03	4.039	0.377
0.246	6.005	4.06	1.425	0.395
0.164	4.013	6.10	0.646	0.401
0.123	3.112	8.13	0.400	0.413
0.098	2.580	10.16	0.308	0.462
0.082	2.123	12.20	0.225	0.500
0.070	1.924	14.23	0.179	0.485
0.062	1.568	16.26	0.131	0.533
0.055	1.280	18.29	0.091	0.558
0.049	1.021	20.33	0.058	0.556
0.045	0.977	22.36	0.050	0.524
0.041	0.923	24.39	0.046	0.541
0.038	0.811	26.42	0.039	0.590
0.035	0.702	28.46	0.030	0.604
0.033	0.603	30.49	0.023	0.626
First Moment				
Regression Statistics				
Multiple R	0.993			
R Square	0.986			
Adjusted R Square	0.914			
Standard Error	0.311			
Observations	15			
	Coefficients	Standard Error	t Statistic	
Intercept	0	#N/A	#N/A	
x1	22.326	0.503	44.407	
HETP				
Regression Statistics				
Multiple R	0.963			
R Square	0.928			
Adjusted R Square	0.923			
Standard Error	0.022			
Observations	15			
	Coefficients	Standard Error	t Statistic	
Intercept	0.366	0.012	30.349	
x1	0.008	0.001	12.970	

Table D-10. Glucose diffusion in packed column of silica gel-100 catalyst (trial # 1).

1/Interstitial velocity,	Corrected first moment,	Regression Statistics			
1/U	μ				
(min/cm)	(min)	Multiple R	0.986		
		R Square	0.972		
0.541	11.109	Adjusted R Square	0.722		
0.270	6.097	Standard Error	0.569		
0.180	4.720	Observations	5		
0.135	3.288				
0.108	2.635		Coefficients	Standard Error	t Statistic
		Intercept	0	#N/A	#N/A
		x1	21.587	0.870	24.805
Interstitial velocity,	Corrected first moment,	Corrected second moment,	HETP		
U	μ	σ^2			
(cm/min)	(min)	$(\text{min})^2$	(cm)		
1.85	11.109	3.045	0.247		
3.70	6.097	0.830	0.223		
5.55	4.720	0.593	0.266		
7.39	3.288	0.264	0.245		
9.24	2.635	0.187	0.269		
Regression Statistics					
Multiple R	0.565				
R Square	0.320				
Adjusted R Square	0.093				
Standard Error	0.018				
Observations	5				
	Coefficients	Standard Error	t Statistic		
Intercept	0.230	0.019	12.340		
x1	0.004	0.003	1.187		

Table D-11. Glucose diffusion in packed column of silica gel-100 catalyst (trial # 2).

1/Interstitial velocity,	Corrected first moment,	Regression Statistics			
1/U	μ				
(min/cm)	(min)	Multiple R	0.986		
		R Square	0.972		
0.541	11.272	Adjusted R Square	0.722		
0.270	6.125	Standard Error	0.573		
0.180	4.790	Observations	5		
0.135	3.292				
0.108	2.735		Coefficients	Standard Error	t Statistic
		Intercept	0	#N/A	#N/A
		x1	21.866	0.877	24.941
Interstitial velocity,	Corrected first moment,	Corrected second moment,	HETP		
U	μ	σ^2			
(cm/min)	(min)	$(min)^2$	(cm)		
1.85	11.272	2.923	0.230		
3.70	6.125	0.804	0.214		
5.55	4.790	0.530	0.231		
7.39	3.292	0.260	0.240		
9.24	2.735	0.186	0.249		
Regression Statistics					
Multiple R	0.779				
R Square	0.608				
Adjusted R Square	0.477				
Standard Error	0.009				
Observations	5				
	Coefficients	Standard Error	t Statistic		
Intercept	0.214	0.010	21.812		
x1	0.003	0.002	2.155		

Table D-12. Glucose diffusion in packed column of silica gel-100 catalyst (trial # 3).

1/Interstitial velocity, 1/U (min/cm)	Corrected first moment, μ (min)	Interstitial velocity, U (cm/min)	Corrected second moment, σ^2 (min)^2	HETP (cm)
0.541	11.402	1.85	1.797	0.138
0.270	6.216	3.70	0.678	0.175
0.180	4.409	5.55	0.324	0.167
0.135	3.526	7.39	0.207	0.166
0.108	2.587	9.24	0.130	0.194
0.090	2.149	11.09	0.100	0.217
0.077	1.905	12.93	0.078	0.216
0.068	1.552	14.78	0.052	0.218
0.060	1.284	16.63	0.042	0.253
0.054	1.066	18.48	0.024	0.213
0.049	0.989	20.33	0.021	0.210
0.045	0.938	22.17	0.020	0.223
0.042	0.808	24.02	0.015	0.235
0.039	0.701	25.87	0.013	0.267
0.036	0.603	27.72	0.010	0.282
First Moment				
Regression Statistics				
Multiple R	0.996			
R Square	0.991			
Adjusted R Square	0.920			
Standard Error	0.271			
Observations	15			
	Coefficients	Standard Error	t Statistic	
Intercept	0	#N/A	#N/A	
x1	21.972	0.398	55.151	
HETP				
Regression Statistics				
Multiple R	0.895			
R Square	0.800			
Adjusted R Square	0.785			
Standard Error	0.018			
Observations	15			
	Coefficients	Standard Error	t Statistic	
Intercept	0.149	0.010	15.042	
x1	0.004	0.001	7.221	

Table D-13. Glucitol diffusion in packed column of HY-zeolite catalyst (trial # 1).

1/Interstitial velocity,	Corrected first moment,	Regression Statistics			
1/U	μ				
(min/cm)	(min)	Multiple R	0.994		
		R Square	0.989		
0.671	17.191	Adjusted R Square	0.739		
0.336	9.281	Standard Error	0.561		
0.224	6.542	Observations	5		
0.168	4.953				
0.134	3.947		Coefficients	Standard Error	t Statistic
		Intercept	0	#N/A	#N/A
		x1	26.503	0.691	38.334
Interstitial velocity,	Corrected first moment,	Corrected second moment,	HETP		
U	μ	σ^2			
(cm/min)	(min)	$(min)^2$	(cm)		
1.49	17.191	20.261	0.686		
2.98	9.281	5.109	0.593		
4.46	6.542	3.411	0.797		
5.95	4.953	1.540	0.628		
7.44	3.947	1.011	0.649		
Regression Statistics					
Multiple R	0.078				
R Square	0.006				
Adjusted R Square	-0.325				
Standard Error	0.090				
Observations	5				
	Coefficients	Standard Error	t Statistic		
Intercept	0.682	0.095	7.206		
x1	-0.003	0.019	-0.136		

Table D-14. Glucitol diffusion in packed column of HY-zeolite catalyst (trial # 2).

1/Interstitial velocity,	Corrected first moment,	Regression Statistics			
1/U	μ				
(min/cm)	(min)	Multiple R	0.995		
		R Square	0.989		
0.671	17.159	Adjusted R Square	0.739		
0.336	9.254	Standard Error	0.546		
0.224	6.520	Observations	5		
0.168	4.921				
0.134	3.907		Coefficients	Standard Error	t Statistic
		Intercept	0	#N/A	#N/A
		x1	26.432	0.672	39.333
Interstitial velocity,	Corrected first moment,	Corrected second moment,	HETP		
U	μ	σ^2			
(cm/min)	(min)	$(\text{min})^2$	(cm)		
1.49	17.159	20.247	0.688		
2.98	9.254	5.072	0.592		
4.46	6.520	3.399	0.800		
5.95	4.921	1.526	0.630		
7.44	3.907	0.996	0.653		
Regression Statistics					
Multiple R	0.064				
R Square	0.004				
Adjusted R Square	-0.328				
Standard Error	0.091				
Observations	5				
	Coefficients	Standard Error	t Statistic		
Intercept	0.682	0.096	7.136		
x1	-0.002	0.019	-0.112		

Table D-15. Glucitol diffusion in packed column of Na-MCM-20 catalyst (trial # 1).

1/Interstitial velocity,	Corrected first moment,	Regression Statistics			
1/U	μ				
(min/cm)	(min)	Multiple R	0.994		
		R Square	0.989		
0.607	13.759	Adjusted R Square	0.739		
0.303	7.865	Standard Error	0.462		
0.202	4.767	Observations	5		
0.152	3.641				
0.121	3.094		Coefficients	Standard Error	t Statistic
		Intercept	0	#N/A	#N/A
		x1	23.431	0.629	37.236
Interstitial velocity,	Corrected first moment,	Corrected second moment,	HETP		
U	μ	σ^2			
(cm/min)	(min)	$(\text{min})^2$	(cm)		
1.65	13.759	4.092	0.216		
3.30	7.865	2.933	0.474		
4.94	4.767	2.671	1.176		
6.59	3.641	2.008	1.515		
8.24	3.094	1.899	1.985		
Regression Statistics					
Multiple R	0.992				
R Square	0.984				
Adjusted R Square	0.978				
Standard Error	0.107				
Observations	5				
	Coefficients	Standard Error	t Statistic		
Intercept	-0.301	0.113	-2.670		
x1	0.278	0.021	13.474		

Table D-16. Glucitol diffusion in packed column of Na-MCM-20 catalyst (trial # 2).

1/Interstitial velocity,	Corrected first moment,	Regression Statistics			
1/U	μ				
(min/cm)	(min)	Multiple R	0.994		
		R Square	0.988		
0.607	13.665	Adjusted R Square	0.738		
0.303	7.875	Standard Error	0.479		
0.202	4.776	Observations	5		
0.152	3.633				
0.121	3.006		Coefficients	Standard Error	t Statistic
		Intercept	0	#N/A	#N/A
		x1	23.311	0.653	35.712
Interstitial velocity,	Corrected first moment,	Corrected second moment,	HETP		
U	μ	σ^2			
(cm/min)	(min)	$(\text{min})^2$	(cm)		
1.65	13.665	3.442	0.184		
3.30	7.875	3.238	0.522		
4.94	4.776	2.423	1.062		
6.59	3.633	2.050	1.553		
8.24	3.006	1.777	1.967		
Regression Statistics					
Multiple R	0.998				
R Square	0.996				
Adjusted R Square	0.994				
Standard Error	0.056				
Observations	5				
	Coefficients	Standard Error	t Statistic		
Intercept	-0.322	0.059	-5.470		
x1	0.279	0.011	25.923		

Table D-17. Glucitol diffusion in packed column of Na-MCM-41 catalyst (trial # 1).

1/Interstitial velocity,	Corrected first moment,	Regression Statistics			
1/U	μ				
(min/cm)	(min)	Multiple R	0.969		
		R Square	0.939		
0.621	13.754	Adjusted R Square	0.689		
0.312	8.295	Standard Error	0.991		
0.207	5.644	Observations	5		
0.156	4.742				
0.125	3.693		Coefficients	Standard Error	t Statistic
		Intercept	0	#N/A	#N/A
		x1	23.859	1.318	18.099
Interstitial velocity,	Corrected first moment,	Corrected second moment,	HETP		
U	μ	σ^2			
(cm/min)	(min)	$(min)^2$	(cm)		
1.61	13.754	5.878	0.311		
3.21	8.295	6.358	0.924		
4.82	5.644	3.555	1.116		
6.42	4.742	3.911	1.739		
8.03	3.693	1.950	1.430		
Regression Statistics					
Multiple R	0.892				
R Square	0.795				
Adjusted R Square	0.727				
Standard Error	0.283				
Observations	5				
	Coefficients	Standard Error	t Statistic		
Intercept	0.188	0.297	0.632		
x1	0.190	0.056	3.411		

Table D-18. Glucitol diffusion in packed column of Na-MCM-41 catalyst (trial # 2).

1/Interstitial velocity,	Corrected first moment,	Regression Statistics			
1/U	μ				
(min/cm)	(min)	Multiple R	0.971		
		R Square	0.944		
0.621	13.737	Adjusted R Square	0.694		
0.312	8.315	Standard Error	0.961		
0.207	5.617	Observations	5		
0.156	4.605				
0.125	3.688		Coefficients	Standard Error	t Statistic
		Intercept	0	#N/A	#N/A
		x1	23.804	1.278	18.628
Interstitial velocity,	Corrected first moment,	Corrected second moment,	HETP		
U	μ	σ^2			
(cm/min)	(min)	$(min)^2$	(cm)		
1.61	13.737	5.911	0.313		
3.21	8.315	6.312	0.913		
4.82	5.617	3.480	1.103		
6.42	4.605	3.620	1.707		
8.03	3.688	2.036	1.497		
Regression Statistics					
Multiple R	0.920				
R Square	0.846				
Adjusted R Square	0.795				
Standard Error	0.246				
Observations	5				
	Coefficients	Standard Error	t Statistic		
Intercept	0.158	0.258	0.613		
x1	0.197	0.048	4.067		

Table D-19. Glucitol diffusion in packed column of silica gel-60 catalyst (trial # 1).

1/Interstitial velocity,	Corrected first moment,	Regression Statistics			
1/U	μ				
(min/cm)	(min)	Multiple R	0.999		
		R Square	0.998		
0.459	16.924	Adjusted R Square	0.748		
0.229	8.945	Standard Error	0.231		
0.153	5.594	Observations	5		
0.115	4.188				
0.092	3.517		Coefficients	Standard Error	t Statistic
		Intercept	0	#N/A	#N/A
		x1	37.255	0.416	89.508
Interstitial velocity,	Corrected first moment,	Corrected second moment,	HETP		
U	μ	σ^2			
(cm/min)	(min)	$(min)^2$	(cm)		
2.18	16.924	15.849	0.553		
4.36	8.945	6.173	0.772		
6.54	5.594	2.229	0.712		
8.71	4.188	1.418	0.808		
10.89	3.517	1.081	0.874		
Regression Statistics					
Multiple R	0.882				
R Square	0.777				
Adjusted R Square	0.703				
Standard Error	0.066				
Observations	5				
	Coefficients	Standard Error	t Statistic		
Intercept	0.540	0.070	7.770		
x1	0.031	0.010	3.234		

Table D-20. Glucitol diffusion in packed column of silica gel-60 catalyst (trial # 2).

1/Interstitial velocity,	Corrected first moment,	Regression Statistics			
1/U	μ				
(min/cm)	(min)	Multiple R	0.999		
		R Square	0.999		
0.459	17.089	Adjusted R Square	0.749		
0.229	8.945	Standard Error	0.201		
0.153	5.595	Observations	5		
0.115	4.205				
0.092	3.378		Coefficients	Standard Error	t Statistic
		Intercept	0	#N/A	#N/A
		x1	37.466	0.363	103.195
Interstitial velocity,	Corrected first moment,	Corrected second moment,	HETP		
U	μ	σ^2			
(cm/min)	(min)	$(\text{min})^2$	(cm)		
2.18	17.089	16.104	0.551		
4.36	8.945	6.207	0.776		
6.54	5.595	2.334	0.746		
8.71	4.205	1.441	0.815		
10.89	3.378	1.076	0.943		
Regression Statistics					
Multiple R	0.918				
R Square	0.843				
Adjusted R Square	0.790				
Standard Error	0.065				
Observations	5				
	Coefficients	Standard Error	t Statistic		
Intercept	0.519	0.068	7.622		
x1	0.038	0.009	4.008		

Table D-21. Glucitol diffusion in packed column of silica gel-100 catalyst (trial # 1).

1/Interstitial velocity,	Corrected first moment,	Regression Statistics			
1/U	μ				
(min/cm)	(min)	Multiple R	0.992		
		R Square	0.984		
0.541	14.638	Adjusted R Square	0.734		
0.270	7.975	Standard Error	0.563		
0.180	5.674	Observations	5		
0.135	4.335				
0.108	3.445		Coefficients	Standard Error	t Statistic
		Intercept	0	#N/A	#N/A
		x1	28.173	0.860	32.742
Interstitial velocity,	Corrected first moment,	Corrected second moment,	HETP		
U	μ	σ^2			
(cm/min)	(min)	$(\text{min})^2$	(cm)		
1.85	14.638	18.104	0.845		
3.70	7.975	4.371	0.687		
5.55	5.674	2.896	0.899		
7.39	4.335	1.892	1.007		
9.24	3.445	0.994	0.838		
Regression Statistics					
Multiple R	0.417				
R Square	0.174				
Adjusted R Square	-0.102				
Standard Error	0.122				
Observations	5				
	Coefficients	Standard Error	t Statistic		
Intercept	0.764	0.128	5.987		
x1	0.017	0.021	0.794		

Table D-22. Glucitol diffusion in packed column of silica gel-100 catalyst (trial # 2).

1/Interstitial velocity,	Corrected first moment,	Regression Statistics			
1/U	μ				
(min/cm)	(min)	Multiple R	0.991		
		R Square	0.982		
0.541	14.611	Adjusted R Square	0.732		
0.270	8.000	Standard Error	0.608		
0.180	5.786	Observations	5		
0.135	4.402				
0.108	3.359		Coefficients	Standard Error	t Statistic
		Intercept	0	#N/A	#N/A
		x1	28.201	0.929	30.346
Interstitial velocity,	Corrected first moment,	Corrected second moment,	HETP		
U	μ	σ^2			
(cm/min)	(min)	$(\text{min})^2$	(cm)		
1.85	14.611	18.051	0.846		
3.70	8.000	4.628	0.723		
5.55	5.786	2.765	0.826		
7.39	4.402	1.609	0.831		
9.24	3.359	1.076	0.954		
Regression Statistics					
Multiple R	0.625				
R Square	0.391				
Adjusted R Square	0.188				
Standard Error	0.074				
Observations	5				
	Coefficients	Standard Error	t Statistic		
Intercept	0.739	0.077	9.537		
x1	0.018	0.013	1.388		

Table D-23. Glucitol diffusion in packed column of silica gel-100 catalyst (trial # 3).

1/Interstitial velocity, 1/U (min/cm)	Corrected first moment, μ (min)	Interstitial velocity, U (cm/min)	Corrected second moment, σ^2 (min)^2	HETP (cm)
0.541	14.420	1.85	4.496	0.216
0.270	7.507	3.70	1.306	0.232
0.180	5.393	5.55	0.740	0.254
0.135	4.100	7.39	0.455	0.270
0.108	3.481	9.24	0.353	0.292
0.090	3.039	11.09	0.283	0.306
0.077	2.677	12.93	0.239	0.334
0.068	2.332	14.78	0.200	0.367
0.060	2.062	16.63	0.172	0.405
0.054	1.948	18.48	0.163	0.429
0.049	1.869	20.33	0.155	0.445
0.045	1.722	22.17	0.142	0.480
0.042	1.593	24.02	0.131	0.516
0.039	1.479	25.87	0.125	0.573
0.036	1.380	27.72	0.111	0.580
First Moment				
Regression Statistics				
Multiple R	0.991			
R Square	0.982			
Adjusted R Square	0.911			
Standard Error	0.456			
Observations	15			
	Coefficients	Standard Error	t Statistic	
Intercept	0	#N/A	#N/A	
x1	28.009	0.671	41.727	
HETP				
Regression Statistics				
Multiple R	0.992			
R Square	0.984			
Adjusted R Square	0.983			
Standard Error	0.016			
Observations	15			
	Coefficients	Standard Error	t Statistic	
Intercept	0.165	0.009	18.997	
x1	0.015	0.001	28.105	

Appendix E: Particle Size Data

Table E-1. Particle size data of HY-zeolite, Na-MCM-20 and Na-MCM-41.

Particle size, d_p (μm)	Weight fraction **(HY-zeolite)**	Weight fraction **(Na-MCM-20)**	Weight fraction **(Na-MCM-41)**
75.00	0.000	0.000	0.000
65.0	0.000	0.000	0.000
55.0	0.000	0.000	0.000
45.0	0.059	0.126	0.000
35.0	0.067	0.241	0.100
25.0	0.055	0.138	0.174
15.0	0.169	0.179	0.301
9.50	0.033	0.027	0.027
8.50	0.033	0.024	0.034
7.50	0.059	0.025	0.034
6.50	0.097	0.031	0.040
5.50	0.122	0.035	0.046
4.50	0.126	0.037	0.052
3.50	0.085	0.049	0.062
2.50	0.049	0.045	0.068
1.50	0.030	0.033	0.043
0.95	0.002	0.010	0.002
0.85	0.003	0.000	0.002
0.75	0.001	0.000	0.002
0.65	0.001	0.000	0.003
0.55	0.001	0.000	0.002
0.45	0.000	0.000	0.002
0.35	0.001	0.000	0.002
0.25	0.000	0.000	0.001
0.15	0.000	0.000	0.001
0.05	0.007	0.000	0.002

Table E-2. Particle size data of silica gel-60 and silica gel-100.

Particle size, d_p (μm)	Weight fraction (**silica gel-60**)	Weight fraction (**silica gel-100**)
100.0	0.000	0.020
95.0	0.000	0.228
85.0	0.000	0.172
75.0	0.085	0.190
65.0	0.295	0.093
55.0	0.254	0.056
45.0	0.103	0.050
35.0	0.046	0.056
25.0	0.033	0.040
15.0	0.001	0.059
9.50	0.012	0.005
8.50	0.022	0.006
7.50	0.030	0.005
6.50	0.033	0.005
5.50	0.030	0.004
4.50	0.009	0.005
3.50	0.027	0.003
2.50	0.001	0.002
1.50	0.014	0.001
0.50	0.005	0.000

Appendix F: Data File Listings

Chromatography Files (ASCII files)

Table F-1. Glucose in HY-zeolite.

Flow rate (mL/min)	0.1	0.2	0.3	0.4	0.5
Trial # 1	RZF1R1	RZF2R1	RZF3R1	RZF4R1	RZF5R1
Trial # 2	RZF1R2	RZF2R2	RZF3R2	RZF4R2	RZF5R2

Table F-2. Glucose in Na-MCM-20.

Flow rate (mL/min)	0.1	0.2	0.3	0.4	0.5
Trial # 1	RM20F1R1	RM20F2R1	RM20F3R1	RM20F4R1	RM20F5R1
Trial # 2	RM20F1R2	RM20F2R2	RM20F3R2	RM20F4R2	RM20F5R2

Table F-3. Glucose in Na-MCM-41.

Flow rate (mL/min)	0.1	0.2	0.3	0.4	0.5
Trial # 1	RM41F1R1	RM41F2R1	RM41F3R1	RM41F4R1	RM41F5R1
Trial # 2	RM41F1R2	RM41F2R2	RM41F3R2	RM41F4R2	RM41F5R2

Table F-4. Glucose in silica gel-60.

Flow rate (mL/min)	0.1	0.2	0.3	0.4	0.5
Trial # 1	RS2F1R1	RS2F2R1	RS2F3R1	RS2F4R1	RS2F5R1
Trial # 2	RS2F1R2	RS2F2R2	RS2F3R2	RS2F4R2	RS2F5R2

Table F-5. Glucose in silica gel-100.

Flow rate (mL/min)	0.1	0.2	0.3	0.4	0.5
Trial # 1	1SF1R1	1SF2R1	1SF3R1	1SF4R1	1SF5R1
Trial # 2	1SF1R2	1SF2R2	1SF3R2	1SF4R2	1SF5R2

Table F-6. Glucitol in HY-zeolite.

Flow rate (mL/min)	0.1	0.2	0.3	0.4	0.5
Trial # 1	SZF1R1	SZF2R1	SZF3R1	SZF4R1	SZF5R1
Trial # 2	SZF1R2	SZF2R2	SZF3R2	SZF4R2	SZF5R2

Table F-7. Glucitol in Na-MCM-20.

Flow rate (mL/min)	0.1	0.2	0.3	0.4	0.5
Trial # 1	SM20F1R1	SM20F2R1	SM20F3R1	SM20F4R1	SM20F5R1
Trial # 2	SM20F1R2	SM20F2R2	SM20F3R2	SM20F4R2	SM20F5R2

Table F-8. Glucitol in Na-MCM-41.

Flow rate (mL/min)	0.1	0.2	0.3	0.4	0.5
Trial # 1	SM41F1R1	SM41F2R1	SM41F3R1	SM41F4R1	SM41F5R1
Trial # 2	SM41F1R2	SM41F2R2	SM41F3R2	SM41F4R2	SM41F5R2

Table F-9. Glucitol in silica gel-60.

Flow rate (mL/min)	0.1	0.2	0.3	0.4	0.5
Trial # 1	SSF1R1	SSF2R1	SSF3R1	SSF4R1	SSF5R1
Trial # 2	SSF1R2	SSF2R2	SSF3R2	SSF4R2	SSF5R2

Table F-10. Glucitol in silica gel-100.

Flow rate (mL/min)	0.1	0.2	0.3	0.4	0.5
Trial # 1	S1SF1R1	S1SF2R1	S1SF3R1	S1SF4R1	S1SF5R1
Trial # 2	S1SF1R2	S1SF2R2	S1SF3R2	S1SF4R2	S1SF5R2

Table F-11. Glucose in silica gel-60, glucose in silica gel-100 and glucitol in silica gel-100 (Trial # 3).

Flow rate (mL/min)	Glucose in silica gel-60	Glucose in silica gel-100	Glucitol in silica gel-100
0.1	NSF1	N1SF1R1	SN1SF1
0.2	NSF2	N1SF2R1	SN1SF2
0.3	NSF3	N1SF3R1	SN1SF3
0.4	NSF4	N1SF4R1	SN1SF4
0.5	NSF5	N1SF5R1	SN1SF5
0.6	NSF6	N1SF6R1	SN1SF6
0.7	NSF7	N1SF7R1	SN1SF7
0.8	NSF8	N1SF8R1	SN1SF8
0.9	NSF9	N1SF9R1	SN1SF9
1.0	NSF10	N1SF10R1	SN1SF10
1.1	NSF11	N1SF11R1	SN1SF11
1.2	NSF12	N1SF12R1	SN1SF12
1.3	NSF13	N1SF13R1	SN1SF13
1.4	NSF14	N1SF14R1	SN1SF14
1.5	NSF15	N1SF15R1	SN1SF15

BET & Pore size Files

Table F-12. BET & pore size distribution data files for 5 catalysts.

Catalyst	N_2 - Analysis	Ar - Analysis
HY-zeolite	Data1.017	Data1.029
Na-MCM-20	Data1.119	Data1.069
Na-MCM-41	Data1.102	Data1.062
silica gel-60	Data1.104	-
silica gel-100	Data1.103	-

Appendix G: Experimental Procedures

Column Packing

1) Weigh the empty column.
2) Sieve the catalyst into the desired range.
3) Put 5 mg catalyst into the column.
4) Tap the column on a hard surface.
5) Do number 3 again until the column is totally filled.
6) Weigh the packed column.

HPLC Preparation

1) Connect the packed column with the HPLC system.
2) Flow HPLC grade water 0.1 mL/min through the column.
3) Heat the column to 70 ^{0}C for 2 hours (under a solvent flow of 0.1 mL/min).
4) Cool the column down to 30 ^{0}C for 12 hours (under a solvent flow of 0.1 mL/min).

Experimental Operation

1) Prepare 50 mg/mL sample solution.
2) Load 20 μL of a sample solution using a syringe.
3) Inject into the column.